Cell Reports

Article

The gut microbiota regulates hypothalamic inflammation and leptin sensitivity in Western diet-fed mice via a GLP-1R-dependent mechanism

Graphical abstract

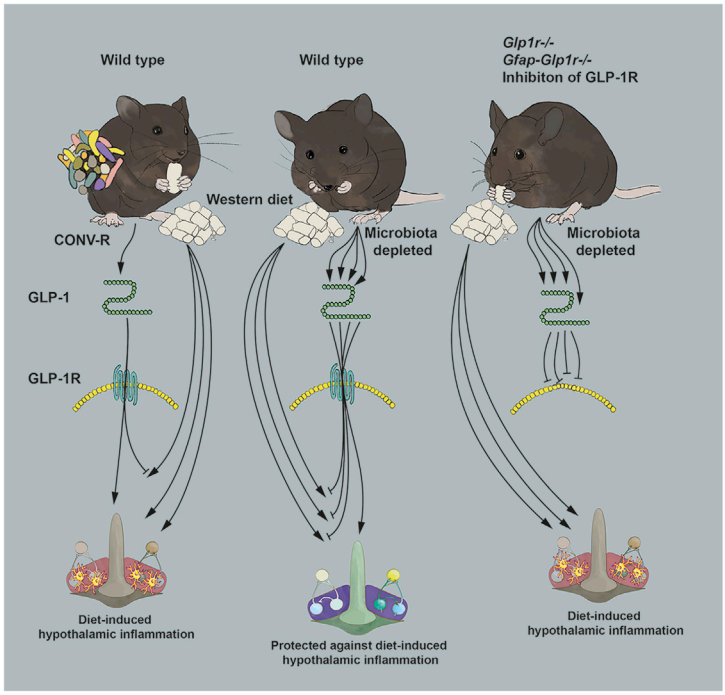

Highlights

- Microbiota-depleted mice are protected from diet-induced hypothalamic inflammation
- Plasma GLP-1 levels are elevated in microbiota-depleted mice
- Inhibition of GLP-1R diminishes the protection against hypothalamic inflammation
- Astrocytes express GLP-1R, and GLP-1R deletion in GFAP$^+$ cells reduces protection

Authors

Christina N. Heiss, Louise Mannerås-Holm, Ying Shiuan Lee, ..., Daniel J. Drucker, Fredrik Bäckhed, Louise E. Olofsson

Correspondence

louise.olofsson@wlab.gu.se

In brief

Feeding a Western diet leads to hypothalamic inflammation, which has been implicated in leptin resistance and weight gain. Heiss et al. show that depletion of the gut microbiota attenuates diet-induced hypothalamic inflammation and enhances leptin sensitivity. Deletion or inhibition of GLP-1R diminishes the protection against diet-induced hypothalamic inflammation.

Heiss et al., 2021, Cell Reports *35*, 109163
May 25, 2021
https://doi.org/10.1016/j.celrep.2021.109163

CellPress

Cell Reports

CellPress
OPEN ACCESS

Article

The gut microbiota regulates hypothalamic inflammation and leptin sensitivity in Western diet-fed mice via a GLP-1R-dependent mechanism

Christina N. Heiss,[1] Louise Mannerås-Holm,[1] Ying Shiuan Lee,[1] Julia Serrano-Lobo,[1] Anna Håkansson Gladh,[1] Randy J. Seeley,[2] Daniel J. Drucker,[3] Fredrik Bäckhed,[1,4,5] and Louise E. Olofsson[1,6,*]

[1]Wallenberg Laboratory, Department of Molecular and Clinical Medicine, Institute of Medicine, University of Gothenburg, 41345 Gothenburg, Sweden

[2]Department of Surgery, University of Michigan Medical School, Ann Arbor, MI 48109, USA

[3]Department of Medicine, Lunenfeld-Tanenbaum Research Institute, Mount Sinai Hospital, University of Toronto, ON M5G 1X5, Canada

[4]Novo Nordisk Foundation Center for Basic Metabolic Research, Section for Metabolic Receptology and Enteroendocrinology, Faculty of Health Sciences, University of Copenhagen, 2200 Copenhagen, Denmark

[5]Department of Clinical Physiology, Region Västra Götaland, Sahlgrenska University Hospital, 41345 Gothenburg, Sweden

[6]Lead contact

*Correspondence: louise.olofsson@wlab.gu.se

https://doi.org/10.1016/j.celrep.2021.109163

SUMMARY

Mice lacking a microbiota are protected from diet-induced obesity. Previous studies have shown that feeding a Western diet causes hypothalamic inflammation, which in turn can lead to leptin resistance and weight gain. Here, we show that wild-type (WT) mice with depleted gut microbiota, i.e., germ-free (GF) and antibiotic-treated mice, have elevated levels of glucagon-like peptide-1 (GLP-1), are protected against diet-induced hypothalamic inflammation, and have enhanced leptin sensitivity when fed a Western diet. Using GLP-1 receptor (GLP-1R)-deficient mice and pharmacological inhibition of the GLP-1R in WT mice, we demonstrate that intact GLP-1R signaling is required for preventing hypothalamic inflammation and enhancing leptin sensitivity. Furthermore, we show that astrocytes express the GLP-1R, and deletion of the receptor in glial fibrillary acidic protein (GFAP)-expressing cells diminished the antibiotic-induced protection against diet-induced hypothalamic inflammation. Collectively, our results suggest that depletion of the gut microbiota attenuates diet-induced hypothalamic inflammation and enhances leptin sensitivity via GLP-1R-dependent mechanisms.

INTRODUCTION

Gut microbes metabolize otherwise indigestible complex carbohydrates, generating short-chain fatty acids (SCFAs), which can be used as energy by the host. Mice lacking a microbiota, i.e., germ-free (GF) and antibiotic (Abx)-treated mice, are lean compared with conventionally raised (CONV-R) mice, partly due to decreased fermentation and absorption of energy from the intestine (Bäckhed et al., 2004; Carvajal-Aldaz et al., 2017; McNeil, 1984). However, GF and Abx-treated mice are also resistant to diet-induced obesity when fed a Western diet containing low amounts of complex carbohydrates, indicating that the gut microbiota directly modifies the host's metabolism (Bäckhed et al., 2007; Cani et al., 2008; Sonnenburg and Bäckhed, 2016).

Leptin is a hormone secreted from the adipose tissue in proportion to the amount of fat in the body and can thus communicate the body's energy stores to the brain (Considine et al., 1996; Schwartz et al., 2000). It acts in the brain to decrease food intake and increase energy expenditure, effects that require signal transducer and activator of transcription 3 (STAT3) signaling (Bates et al., 2003). GF mice exhibit an enhanced anorexigenic response to leptin compared with CONV-R mice (Schéle et al., 2013). However, because increased adiposity and elevated circulating leptin levels can cause leptin resistance (Pan and Myers, 2018), it remains unclear how GF mice acquire enhanced leptin sensitivity.

Feeding a Western diet leads to hypothalamic inflammation, which is characterized by increased expression of inflammatory mediators, neuronal injury, as well as reactive gliosis, i.e., recruitment, proliferation, and activation of microglia and astrocytes (Thaler et al., 2012). Hypothalamic inflammation occurs prior to weight gain (Thaler et al., 2012) and has thus been suggested to contribute to rather than being a consequence of weight gain, potentially by causing leptin resistance (Thaler et al., 2013). Microglia activation has a central role in diet-induced hypothalamic inflammation, and depletion of the microglia from the mediobasal hypothalamus reduces the inflammation and improves leptin sensitivity (Valdearcos et al., 2014). Intriguingly, the gut microbiota regulates microglia maturation and function (Erny et al., 2015), but the mechanism involved remains unclear.

The hormone glucagon-like peptide-1 (GLP-1), which is mainly produced in the intestinal L cells and in the brainstem (Drucker, 2007), has anti-inflammatory and neuroprotective effects

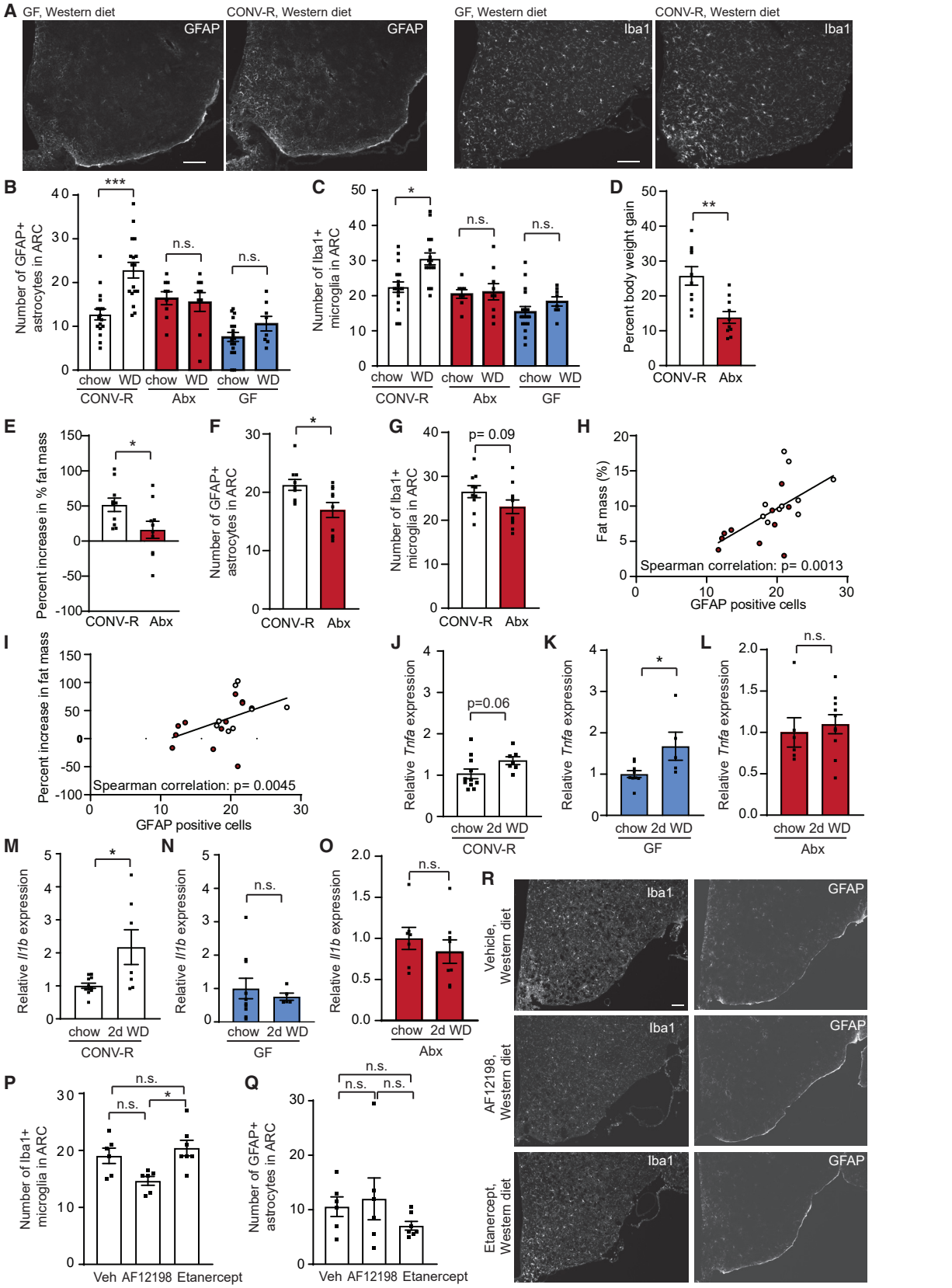

(legend on next page)

(Hölscher, 2014). Microbially produced SCFAs increase GLP-1 plasma levels in rodents via a GPR43-dependent mechanism (Psichas et al., 2015). However, SCFA deficiency in GF and Abx-treated mice, which leads to energy-deprived colonocytes (Donohoe et al., 2012), also increases colonic *Gcg* expression, as well as circulating GLP-1 levels (Wichmann et al., 2013). Administration of SCFAs decreases *Gcg* expression in colon tissue from GF mice *ex vivo*, and a high-fat diet normalizes colonic *Gcg* expression in GF mice, supporting the idea that the energy availability regulates colonic *Gcg* expression (Wichmann et al., 2013). However, it is unclear whether the circulating levels of GLP-1 remain elevated in high-fat diet-fed GF and Abx-treated mice and whether gut microbes indirectly modulate microglia function via GLP-1. Here we determined that the gut microbiota regulates diet-induced hypothalamic inflammation and leptin sensitivity via a GLP-1 receptor (GLP-1R)-dependent mechanism.

RESULTS

Mice lacking a microbiota are protected from diet-induced hypothalamic inflammation

Feeding CONV-R mice a high-fat diet (>40% of calories from fat) causes hypothalamic inflammation, and such inflammation can impair leptin signaling leading to weight gain (Thaler et al., 2013; Valdearcos et al., 2014). Because mice lacking a gut microbiota are protected from diet-induced obesity, we hypothesized that these mice are protected against diet-induced hypothalamic inflammation. We used a short-term high-fat and high-sucrose Western diet intervention (40% of calories from fat) to determine differences in the initial inflammatory response and to focus on the response that could causally contribute to rather than be a secondary consequence of more pronounced weight gain in CONV-R mice compared with mice lacking a microbiota. CONV-R mice fed a Western diet for 1 week developed hypothalamic gliosis with an increased number of glial fibrillary acidic protein (GFAP)-positive astrocytes and ionized calcium-binding adapter molecule 1 (Iba1)-positive microglia in the hypothalamic arcuate nucleus (ARC; Figure S1A) compared with chow-fed CONV-R mice (Figures 1A–1C). In contrast, we did not observe increased numbers of GFAP-positive astrocytes and Iba1-positive microglia in 1-week Western diet-fed GF or Abx-treated mice (Figures 1A–1C). Furthermore, the microglia in Western diet-fed mice with depleted gut microbiota exhibited a less activated morphology with decreased cell body area and increased cell body circularity compared with Western diet-fed CONV-R mice (Figures S1B–S1D). Depletion of the gut microbiota after Abx treatment was confirmed by determining the number of colony-forming units in cecal content from CONV-R and Abx-treated mice under anaerobe or aerobe culture (Figures S1E–S1G). Moreover, Abx treatment led to reduced SCFA levels in the cecum (Figures S1H–S1K), suggesting that the Abx treatment decreased the fermenting capacity of the gut microbiota. The body weight did not differ between the CONV-R, Abx-treated, and GF mice (Figure S1L). However, GF mice fed a Western diet for 1 week gained less weight compared with CONV-R mice (Figure S1M). To determine whether the difference in weight gain could explain the difference in diet-induced gliosis, we performed further analyses of CONV-R mice with similar weight gain as GF mice. In this subgroup of weight gain-matched CONV-R mice, 1 week of feeding a Western diet also increased the number of GFAP-positive astrocytes and Iba1-positive microglia in ARC (Figures S1N and S1O). These results suggest that Western diet-induced gliosis in CONV-R mice occurs prior to weight gain, and that the difference between CONV-R mice and mice lacking a microbiota is not due to differences in weight gain.

To determine whether hypothalamic gliosis correlates with diet-associated increases in body weight and fat mass, we fed CONV-R and Abx-treated mice a Western diet for 4 weeks. Prolonged Western diet feeding led to greater body weight gain and fat mass in CONV-R mice compared with Abx-treated mice (Figures 1D and 1E). This was accompanied by increased numbers of GFAP-positive astrocytes, as well as by a trend of increased numbers of Iba1-positive microglia in ARC from CONV-R compared with Abx-treated mice (Figures 1F and 1G). There was no correlation between number of microglia in ARC and changes in body weight or fat mass at the end of the 4 weeks (data not shown). Although there was no significant correlation between the number of astrocytes, weight gain, or body weight at the end of the 4 weeks, the number of astrocytes correlated with fat mass, as well as relative increase in fat mass during the study (Figures 1H and 1I).

To determine whether the diet-induced hypothalamic gliosis was accompanied by increased inflammatory gene expression, we analyzed *Tnfa*, *Il1b*, and *Il6* gene expression in the hypothalamus of CONV-R, GF, and Abx-treated mice. Although *Tnfa* expression was not altered in Abx-treated mice after 2 days of feeding a Western diet, it was increased in GF mice and trended

Figure 1. Mice lacking a microbiota are protected from diet-induced hypothalamic inflammation

Conventionally raised (CONV-R), germ-free (GF), and antibiotic (Abx)-treated mice were given 1 week of chow or Western diet (WD). Mice were perfused, and hypothalamic sections were prepared and stained for the astrocyte marker GFAP and the microglia marker Iba1.

(A–C) The number of GFAP- (A and B) and Iba1-positive cells (A and C) were determined in wild-type (WT) mice. n = 8–17 per group.

(D–I) CONV-R and Abx-treated mice were fed a WD for 4 weeks.

(D–G) Body weight gain, fat mass gain, and numbers of Iba1- and GFAP-positive cells were determined (n = 10 per group).

(H and I) Correlations between GFAP-positive cells and fat mass (%) and percent increase in fat mass are shown. Open circles indicate CONV-R, and red circles indicate Abx-treated mice.

(J–O) Hypothalamic *Tnfα* (J–L) and *Il1b* (M–O) gene expressions were analyzed in CONV-R, GF, and Abx-treated mice given a chow diet or a WD for 2 days (n = 5–11 per group). IL, interleukin; TNF-α, tumor necrosis factor alpha.

(P–R) The number of Iba1-positive microglia (P and R) and GFAP-positive astrocytes (Q and R) in hypothalamic arcuate nucleus (ARC) from WD-fed WT mice treated with vehicle (Veh), AF12198, or etanercept (n = 6–7 mice per WD-fed group).

*p < 0.05, **p < 0.01, ***p < 0.001 as determined by Mann-Whitney rank test (B–G and J–O), Spearman correlation (H and I), or Kruskal-Wallis test (P–Q). Data are presented as mean ± SEM. Each data point in (B), (C), (F), (G), and (J)–(Q) represents one mouse and the mean of at least two measurements. Scale bar: 100 μm. See also Figure S1.

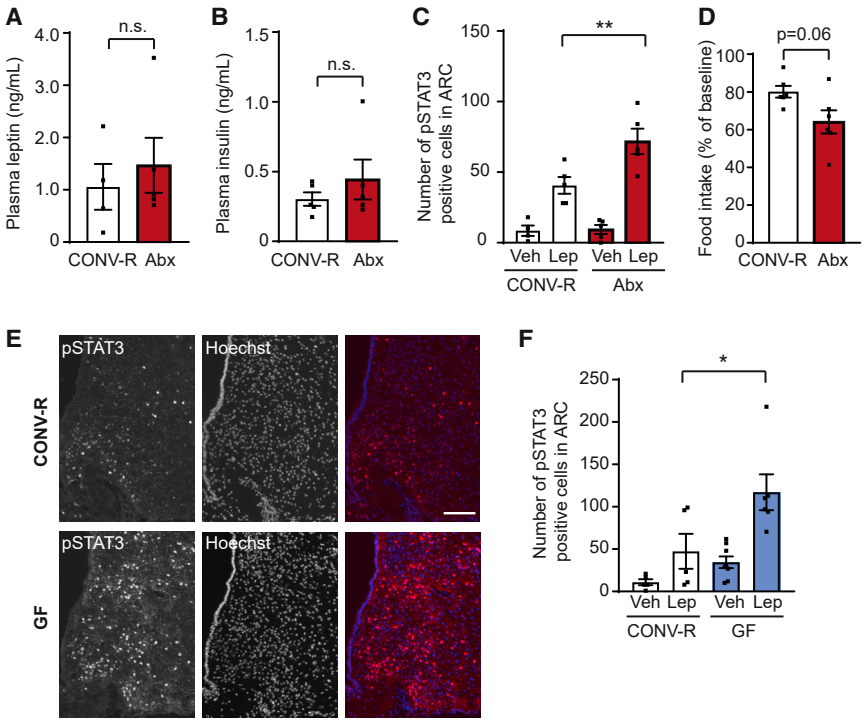

Figure 2. Microbiota deprivation enhances phosphorylated signal transducers and activators of transcription 3 (pSTAT3) signaling upon leptin injection

(A and B) Plasma Lep and insulin levels in body weight-matched WD-fed CONV-R and Abx-treated mice (n = 4–5).

(C) pSTAT3 in the ARC was determined upon vehicle (Veh) or leptin (Lep) injection in CONV-R and Abx-treated mice fed a WD for 1 week (n = 4–5 per group).

(D) Twenty-four-hour food intake was measured in response to Lep injections in WD-fed mice treated with Abx or placebo (n = 6 per group).

(E and F) Lep-induced pSTAT3 signaling was also determined in CONV-R and GF mice fed a WD for 1 week (n = 5–8 per group).

Scale bar: 100 μm. *p < 0.05, **p < 0.01 as determined by Mann-Whitney. Data are presented as mean ± SEM. Each data point in (A)–(D) and (F) represents one mouse and the mean of at least two measurements.

See also Figure S2.

higher in CONV-R mice (Figures 1J–1L). In contrast, hypothalamic *Il1b* expression was increased in CONV-R and not in GF or Abx-treated mice after feeding a Western diet for 2 days (Figures 1M–1O). The levels of *Il1b* and *Tnfa* mRNA in CONV-R, GF, or Abx-treated mice did not differ between chow-fed versus Western diet-fed mice after 1 week (Figures S1P–S1U). Hypothalamic *Il6* expression did not differ in chow- or Western diet-fed CONV-R mice (data not shown). To determine whether interleukin (IL)-1β or tumor necrosis factor alpha (TNF-α) is required for the initial diet-induced hypothalamic inflammation, we treated Western diet-fed CONV-R mice with vehicle, an interleukin-1 receptor (IL-1R) antagonist, or a TNF inhibitor. Administration of the TNF inhibitor etanercept did not affect the number of astrocytes or microglia compared with vehicle (Figures 1P–1R). The number of microglia trended lower in AF12198-treated mice compared with vehicle-treated mice (Figure 1P). These results suggest that IL-1β could potentially play a role in the initial hypothalamic inflammatory response to feeding a Western diet. Taken together, our results indicate that depletion of the microbiota reduces Western diet-induced hypothalamic inflammation.

Microbiota deprivation enhances pSTAT3 signaling upon leptin injection

Because mice lacking a gut microbiota are protected against diet-induced hypothalamic inflammation, we next determined whether these mice also exhibit enhanced leptin sensitivity. It has previously been shown that the gut microbiota suppresses the anorectic effects of leptin in chow-fed rodents (Schéle et al., 2013). However, part of this effect can be due to differences in adiposity and circulating leptin levels. We have previously shown that GF mice are leaner and have reduced circulating leptin levels compared with CONV-R mice, which strongly correlated with adiposity (Bäckhed et al., 2004), suggesting that the reduced leptin levels in GF mice are a result of reduced fat mass. In contrast, studies with certain Abx treatments demonstrated reduced levels of leptin independent of fat mass, suggesting overlapping mechanisms (Wang et al., 2018; Zarrinpar et al., 2018). Considering that our Abx cocktail and treatment regimen differs from these studies, we determined the circulating leptin levels in mice treated with our Abx regimen. Plasma leptin and insulin levels did not differ in weight-matched CONV-R and Abx-treated mice (Figures 2A and 2B). To determine whether mice lacking a gut microbiota have improved leptin sensitivity that could contribute to the protection against diet-induced obesity, we studied weight-matched CONV-R, 10-day Abx-treated, and GF mice fed a Western diet for 1 week (Figure S2A). A 10-day Abx treatment in CONV-R mice led to increased leptin-induced phosphorylation of STAT3 (pSTAT3) in the ARC (Figures 2C and S2B), as well as to a slightly enhanced anorexic effect in response to leptin injection compared with CONV-R mice (Figure 2D). Average decrease in food intake after leptin injection trended lower in Abx-treated mice versus CONV-R controls (35.9% versus 19.9%; p = 0.06; Figure 2D). Similar to the Abx-treated mice, GF mice exhibited increased pSTAT3 in the ARC upon leptin injection compared with CONV-R mice (Figures 2E and 2F). Together, these results indicate that GF and Abx-treated mice exhibit enhanced leptin sensitivity, and that this effect is independent of body weight and circulating leptin levels.

Functional GLP-1R signaling is required for the protection against diet-induced hypothalamic inflammation and the improved leptin sensitivity in mice with depleted gut microbiota

GF and Abx-treated mice have elevated circulating levels of the incretin hormone GLP-1 when fed a chow diet (Wichmann et al.,

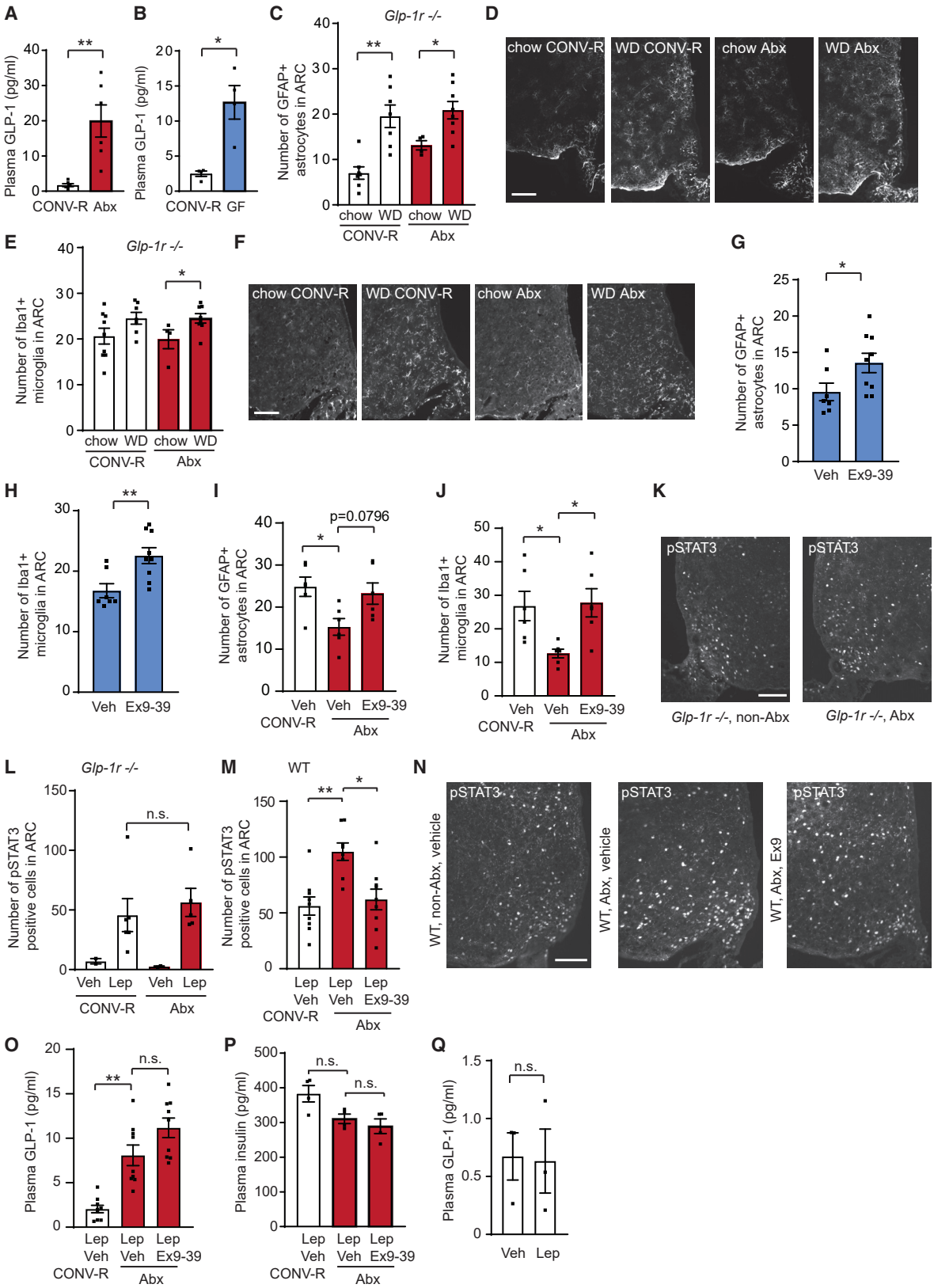

(legend on next page)

2013; Zarrinpar et al., 2018). Because GLP-1 has anti-inflammatory and neuroprotective effects (Hölscher, 2014), and GLP-1 and leptin signaling is closely connected (Kanoski et al., 2015; Shirazi et al., 2013), we hypothesized that the protection against diet-induced hypothalamic inflammation and the enhanced leptin response in mice with depleted gut microbiota are mediated by GLP-1. To test this hypothesis, we first measured colonic *Gcg* expression and GLP-1 concentration in plasma from mice fed a Western diet for 1 week. Colonic *Gcg* expression was increased in chow-fed GF mice compared with CONV-R mice (Figure S3A). Feeding a Western diet decreased the colonic *Gcg* expression in GF mice ($p = 0.0061$), but it remained slightly elevated compared with Western diet-fed CONV-R mice ($p = 0.016$; Figure S3A). Abx-treated and GF mice had higher circulating levels of GLP-1 compared with CONV-R mice after 1 week of feeding a Western diet (Figures 3A and 3B). Plasma GLP-1 levels were also elevated in Abx-treated mice compared with the CONV-R mice after 4 weeks of Western diet feeding (Figure S3B). To determine whether the microbiota modulates the L cell response to nutrient stimuli, we measured circulating GLP-1 levels in vena porta from CONV-R and GF mice before and after an oral glucose challenge. The circulating GLP-1 levels remained elevated in the GF mice after the oral glucose challenge (Figure S3C). Furthermore, the circulating GLP-1 levels in vena porta were higher in fed and 4-h-fasted GF mice compared with CONV-R mice (Figure S3D), consistent with previous observations (Wichmann et al., 2013). Altogether, these results suggest that the microbiota does not acutely modulate the L cell response to nutrient stimuli. Next, we treated GLP-1R-deficient mice with Abx or placebo for 10 days and challenged them with a Western diet for the last 7 days of treatment. In contrast with the wild-type (WT) mice, Abx treatment did not protect GLP-1R-deficient mice from diet-induced hypothalamic gliosis. The number of Iba1-positive microglia and GFAP-positive astrocytes increased after 1 week of Western diet feeding in GLP-1R-deficient mice (Figures 3C–3F and S3E). Furthermore, in contrast with the WT mice, Abx treatment in Western diet-fed GLP-1R-deficient mice did not lead to a less activated microglia morphology (Figures S3F and S3G). Moreover, short-term administration of the GLP-1R antagonist Exendin 9-39 (Ex9-39) via subcutaneously implanted osmotic pumps in weight-matched, 1-week Western diet-fed GF WT mice resulted in an increased diet-induced hypothalamic gliosis (Figures 3G, 3H, S3H, and S3I). There were no differences in levels of SCFAs in cecum or levels of GLP-1 in plasma from the vena cava between the mice administered with Ex9-39 or vehicle (Figures S3J and S3K). Similar to findings in the GF mice, Ex9-39 administration in Abx-treated mice led to an increased number of microglia and astrocytes in ARC compared with vehicle administration (Figures 3I, 3J, S3L, and S3M).

Next, we determined whether Abx treatment improved leptin sensitivity in GLP-1R-deficient mice. In contrast with the enhanced leptin responsivity induced by Abx treatment in WT mice (Figure 2C), Abx treatment in Western diet-fed GLP-1R-deficient mice did not enhance the leptin response (Figures 3K and 3L). Furthermore, administration of Ex9-39 via subcutaneously implanted pumps in weight-matched, 1-week Western diet-fed WT mice abolished the enhanced leptin response induced by Abx treatment (Figures 3M, 3N, and S3L). In the Ex9-39-treated mice, Abx treatment led to an increase in the circulating GLP-1 levels but no change in circulating insulin levels (Figures 3O and 3P). Weight gain and body fat did not differ between the groups (Figures S3N–S3P), but the cecum was enlarged in both groups of Abx-treated mice (Figure S3Q). Because leptin has been shown to regulate GLP-1 secretion from the intestine in fasted mice (Anini and Brubaker, 2003), we determined whether leptin exposure directly increases the circulating GLP-1 levels in our experiment. Mice were injected with leptin or saline, and circulating GLP-1 levels were measured 45 min after injection. The GLP-1 plasma levels did not differ between mice injected with saline or leptin, indicating that short-term leptin exposure in Western diet-fed mice does not affect the circulating GLP-1 levels (Figure 3Q). Taken together, these results suggest that deprivation of the gut microbiota protects against diet-induced hypothalamic inflammation and enhances the hypothalamic leptin response via GLP-1R-dependent mechanisms.

Deletion of GLP-1R in GFAP-expressing cells diminishes Abx-mediated protection against diet-induced hypothalamic inflammation

To determine whether GLP-1 can act directly on microglia or astrocytes in the hypothalamus, we first examined whether

Figure 3. Functional GLP-1 receptor (GLP-1R) signaling is required for protection against diet-induced hypothalamic inflammation and the improved leptin sensitivity in mice with depleted gut microbiota

(A and B) GLP-1 was measured in vena cava plasma from CONV-R and Abx-treated C57BL/6J mice (A; n = 6 per group) and in CONV-R and GF Swiss Webster male mice (B; n = 4–5 per group).

(C–F) The numbers of GFAP-positive astrocytes (C and D) and Iba1-positive microglia (E and F) in ARC from chow- or WD-fed GLP-1R-deficient mice treated with Abx or placebo were determined (n = 4–9 per group). Scale bars: 100 μm.

(G and H) The numbers of GFAP-positive astrocytes (G) and Iba1-positive microglia (H) were determined in WD-fed GF mice administrated with Veh or Exendin 9-39 (Ex9-39; n = 7–9 per group).

(I and J) The numbers of Iba1- and GFAP-positive cells in ARC were determined in WD-fed WT mice treated with Abx or placebo while administrated with Veh or Ex9-39 (n = 6 mice per group).

(K and L) The number of pSTAT3-positive cells in the ARC upon Lep injection was determined in body weight-matched, WD-fed GLP-1R-deficient mice treated with Abx or placebo for 10 days (n = 5–6 mice per Lep-injected group). Scale bar: 100 μm.

(M and N) The number of pSTAT3-positive cells in ARC was determined upon Lep injection in WD-fed WT mice treated with Abx or placebo while administrated with Veh or Ex9-39 (n = 8–9 mice per group). Scale bar: 100 μm.

(O and P) Plasma GLP-1 and insulin in mice treated with Abx or placebo while administrated with Veh or Ex9-39.

(Q) Circulating GLP-1 levels in mice injected with saline or Lep (3 mg/kg) 45 min before killing the mice (n = 3).

*$p < 0.05$, **$p < 0.01$ as determined by Mann-Whitney rank test (A–H, L, and Q) or by Kruskal-Wallis test (I, J, M, O, and P). Data are presented as mean ± SEM. Each data point in (A)–(C), (E), (G), (H)–(J), (L), (M), and (O)–(Q) represents one mouse and the mean of at least two measurements.

See also Figure S3.

microglia and astrocytes express GLP-1R. Using CONV-R WT, GF WT, and CONV-R *Glp1r*$^{-/-}$ mice, we showed that the GLP-1R antibody specifically recognizes GLP-1R (Figure S4A). Due to incompatible antibodies, we used ROSA mTmG reporter mice bred with mice expressing tamoxifen-inducible Cre under the *Cx3cr1* promoter to determine whether microglia express GLP-1R. These mice express EGFP in Cre-expressing cells after tamoxifen injection and thereby mark the microglia, which we confirmed with immunofluorescence using an antibody against Iba1 (Figure S4B). Twelve sections from four 1-week Western diet-fed mice were analyzed, and none of the EGFP-positive microglia cells expressed GLP-1R (Figure S4C). In contrast, a subset of the hypothalamic astrocytes expressed GLP-1R (Figures 4A–4D and S4D). *Glp1r*$^{-/-}$ mice were used as a control, and no GLP-1R staining was observed in hypothalamic astrocytes in these mice (Figure S4E). To determine whether GLP-1R signaling in GFAP-expressing cells mediates the anti-inflammatory effects, we generated mice with tamoxifen-induced deletion of the GLP-1R specifically in GFAP-expressing cells (*Gfap-Glp1r*$^{-/-}$) and confirmed that these mice have reduced expression of GLP-1R in the astrocytes upon tamoxifen injections (Figures 4E and S4F). In contrast, the total number of GLP-1R-positive cells in ARC did not differ between the WT and mutant mice (Figure 4F). To further validate the functional response of GLP-1R deletion in astrocytes, we injected 12-h fasted chow-fed WT and *Gfap-Glp1r*$^{-/-}$ mice with vehicle or the GLP-1R agonist Exendin-4 (Ex4). Using a confocal microscope, we detected c-*fos* immunoreactivity in a majority of the astrocytes in ARC from Ex4-injected WT mice (Figure S4G). Although Ex4 injection led to an increased percent of GFAP-positive astrocytes that were positive for c-*fos* compared with vehicle injection in WT mice, this response was diminished in *Gfap-Glp1r*$^{-/-}$ mice (Figures 4G and S4H), consistent with functional depletion of GLP-1R in astrocytes. To determine whether GLP-1R signaling in GFAP-expressing cells mediates the anti-inflammatory effect of Abx treatment, we treated *Gfap-Glp1r*$^{-/-}$ and control mice with placebo or Abx while fed a Western diet. Abx treatment protected WT mice from Western diet-induced hypothalamic gliosis (Figures 4H and 4I). In contrast, deletion of GLP-1R in GFAP-positive cells diminished the effects of Abx on both astrocytes and microglia. Moreover, although Abx treatment in WT mice led to less activated microglia morphology, Abx treatment did not change the morphology of the microglia in the *Gfap-Glp1r*$^{-/-}$ mice (Figures 4J and 4K). Together, these results suggest that GLP-1 can act on astrocytes to decrease the early diet-induced hypothalamic inflammation.

DISCUSSION

In this study, we showed that the gut microbiota modulates diet-induced hypothalamic inflammation and leptin sensitivity via a GLP-1R-dependent mechanism. We demonstrated that Western diet-fed GF and Abx-treated WT mice are protected against diet-induced hypothalamic inflammation and have enhanced response to leptin compared with CONV-R mice, effects that are abolished in GLP-1R-deficient mice. Furthermore, we show that astrocytes express the GLP-1R, and that deletion of the receptor specifically in GFAP-expressing cells diminishes the Abx-mediated protection against diet-induced hypothalamic gliosis. These effects may contribute to protecting GF and Abx-treated mice against diet-induced obesity.

Microglia are the macrophages of the brain and orchestrate the inflammatory process and neuronal stress in response to saturated fatty acids in the hypothalamus (Valdearcos et al., 2014). The gut microbiota is crucial for microglia maturation and activation (Erny et al., 2015). GF and 4-week Abx-treated mice exhibit immature microglia, indicating that the microglia need continuous stimulation from the gut microbiota to remain mature. Administration of SCFAs to GF mice via drinking water restores the immature microglia phenotype (Erny et al., 2015). However, the signaling pathway(s) linking microbes and microglia is not established. Notably, GF and Abx-treated mice have high circulating levels of GLP-1, and SCFA stimulation of the proximal colon from GF mice leads to decreased *Gcg* expression (Wichmann et al., 2013). Our results show that mice lacking a microbiota are protected against diet-induced hypothalamic microgliosis via a GLP-1R-dependent mechanism. Collectively, these finding suggest that the gut microbes modulate microglia maturation and activation in part via GLP-1R signaling.

We observed an early upregulation of hypothalamic *Il1b* and *Tnfa* gene expression in CONV-R mice in response to feeding a Western diet. Unexpectedly, this upregulation was transient, and hypothalamic *Il1b* and *Tnfa* expression after 1 and 4 weeks of feeding a Western diet did not differ from the chow-fed mice. Previous studies have shown a similar expression pattern (Baufeld et al., 2016), suggesting that these inflammatory mediators have a more important role in the early than in the later inflammatory response. This is supported by the well-known role of IL-1 and TNF-α in the acute phase of inflammation (Lawrence et al., 2002). The body's natural response to resolve inflammation, by production of anti-inflammatory mediators (Lawrence et al., 2002), could potentially lead to the decreased hypothalamic *Il1b* and *Tnfa* expression observed at the 1- and 4-week time points compared with after 2 days of Western diet feeding. This is supported by results showing that prolonged exposure to a high-fat diet leads to increased anti-inflammatory gene expression in the hypothalamus (Baufeld et al., 2016).

GLP-1 is derived from the proglucagon (*Gcg*) gene in the gastrointestinal tract and in the brain and is post-translationally modified and cleaved into the biologically active forms, GLP-1 (7-36) amide and GLP-1 (7-37) (Müller et al., 2019). Active GLP-1 is quickly degraded by the enzyme dipeptidyl peptidase 4 (DPP-4) when entering the circulation, with a half-life of less than 2 min (Müller et al., 2019). It has therefore been questioned whether circulating GLP-1 reaches the brain or if most of the central effects of GLP-1 are mediated by GLP-1 produced in the brain or peripheral GLP-1 acting on vagal afferents in the lamina propria or enteric nerves in the intestinal wall. Previous studies suggest that only a small portion of GLP-1 escapes degradation by DPP-4 and by the liver (Müller et al., 2019), which is supported by our active GLP-1 measurements in the vena cava. The observed plasma GLP-1 levels in the vena cava are approximately 10% of the concentration in the vena porta (Wichmann et al., 2013). A previous study used subdiaphragmatic vagal deafferentations to determine the role of the vagal afferents in mediating the effects of GLP-1. Although vagotomy attenuated

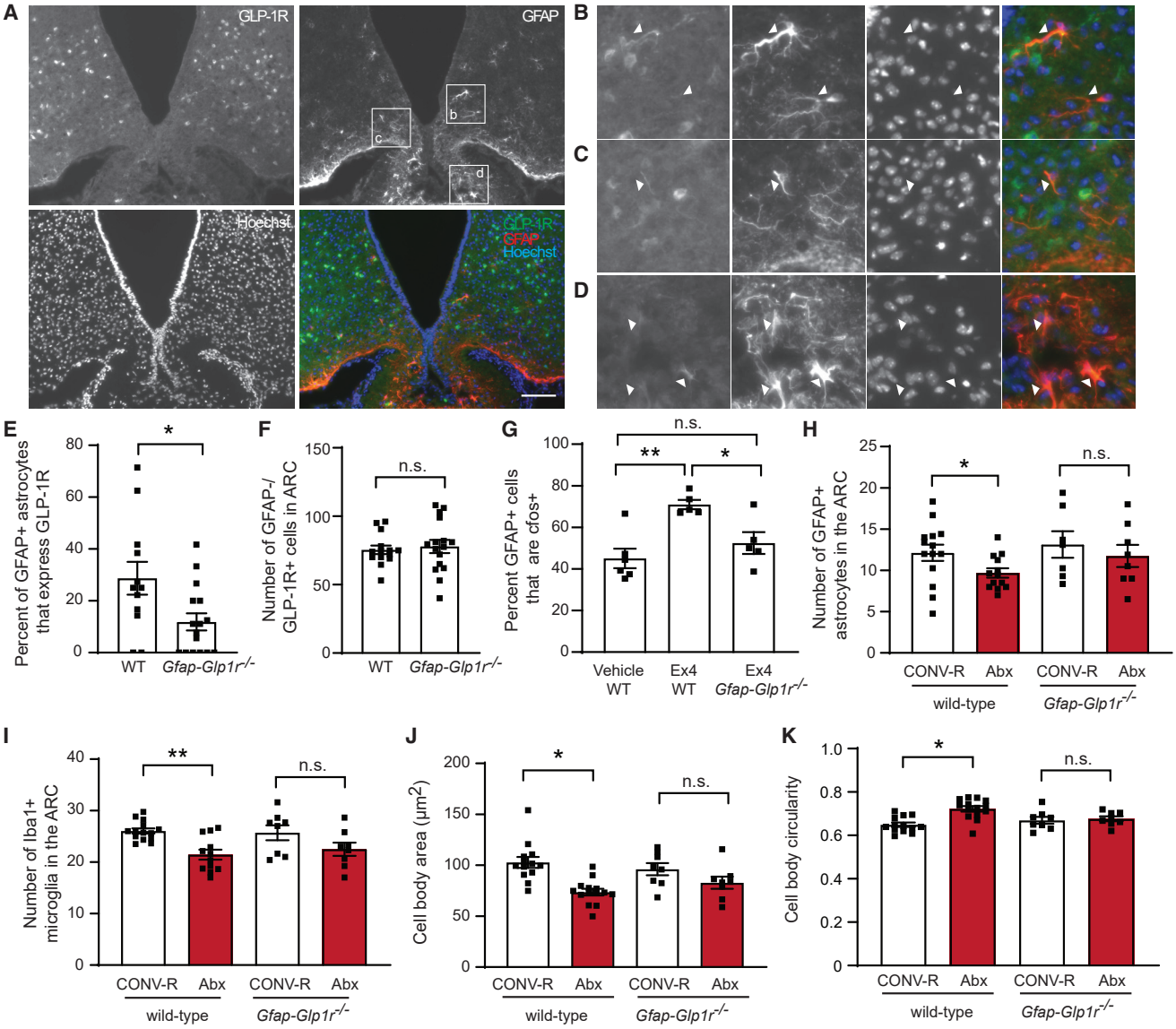

Figure 4. Deletion of GLP-1R in GFAP-expressing cells diminishes Abx-mediated protection against diet-induced hypothalamic inflammation

(A–D) Hypothalamic sections from WT mice were stained using GLP-1R and GFAP antibodies. Co-localization between the astrocytic marker GFAP and the GLP-1R was observed in the hypothalamus.

(B–D) Panels represent inserts in (A). Scale bar: 100 μm.

(E) Mice expressing floxed *Glp-1r* were bred with mice expressing tamoxifen-induced Cre under the Gfap promoter. Percent of GFAP-positive astrocytes in WT and *Gfap-Glp1r*$^{-/-}$ mice that express GLP-1R after tamoxifen injection was measured (n = 12–16 per group).

(F) Numbers of GFAP-negative/GLP-1R-positive cells were determined per hemi-ARC (n = 12–16 per group).

(G) Ex4-induced c-*fos* in ARC from WT and *Gfap-Glp1r*$^{-/-}$ mice (n = 5–6 per group).

(H and I) *Gfap-Glp1r*$^{-/-}$ and WT mice were given a WD for 1 week while treated with Abx or placebo. The numbers of GFAP-positive astrocytes (H) and Iba1-positive microglia (I) were determined in the arcuate nucleus (n = 7–14 per group).

(J and K) Microglia morphology was measured.

*$p < 0.05$, **$p < 0.01$ as determined by Mann-Whitney rank test (E, F, and H–K) or by Kruskal-Wallis test (G). Data are presented as mean ± SEM. Each data point in (E)–(K) represents one mouse and the mean of at least two measurements.

See also Figure S4.

the GLP-1-mediated effects on meal size when GLP-1 was administrated via the intraperitoneal route, vagotomy had no effect when GLP-1 was infused into the hepatic portal vein (Rüttimann et al., 2009), suggesting that intravenous GLP-1 does not require afferent nerves to exert its effects on food intake. The arcuate nucleus is uniquely localized next to the

median eminence, a circumventricular organ, and several studies have shown that the arcuate nucleus of the hypothalamus lacks a complete blood-brain barrier (Langlet et al., 2013; Mullier et al., 2010; Olofsson et al., 2013; Yulyaningsih et al., 2017). Cells located in this region readily respond to circulating substances including hormones (Olofsson et al., 2013), suggesting that GLP-1 that escapes degradation can easily access this region. Altogether, these studies suggest that GLP-1 can act directly on some cells in the mediobasal hypothalamus.

Previous studies have found that microglia and astrocytes can express the GLP-1R (Lee et al., 2018; Timper et al., 2020), suggesting that GLP-1 can exert a direct anti-inflammatory effect on these cells in the brain. In contrast, we observed GLP-1R expression only in astrocytes and not in microglia within the hypothalamus. Using RNAscope-based *in situ* hybridization, as well as assessment of fluorescently labeled GLP-1R agonist uptake, a recent study revealed site-specific expression of GLP-1R in astrocytes. Astrocytes in hypothalamic ARC and paraventricular nucleus (PVN) expressed the receptor, while there was no GLP-1R expression detectable in astrocytes in the nucleus accumbens (Timper et al., 2020). Using a protocol similar to that used in this study to specifically delete GLP-1R in GFAP-expressing astrocytes in adult mice, they showed that approximately 35% of the GFAP-positive cells in ARC from WT mice had visible uptake of fluorescence-labeled GLP-1R agonist, and tamoxifen-induced deletion of the GLP-1R in GFAP-expressing cells reduced this number to just less than 10% (Timper et al., 2020). Consistent with these findings, we found that 29% of the GFAP-positive cells in ARC from WT mice were also positive for GLP-1R, while this number was only 12% in mice with specific deletion of GLP-1R in GFAP-positive cells. Moreover, Timper et al. (2020) found that GLP-1R signaling is required for maintaining mitochondrial integrity and function in hypothalamic astrocytes, and depleting GLP-1R signaling in these cells induced a cellular stress response. Our current results indicate that GLP-1R signaling in astrocytes mediates at least some of the anti-inflammatory effects mediated by GLP-1. In line with our results, several previous studies suggest that GLP-1 and GLP-1R agonists have anti-inflammatory properties and neuroprotective effects, and that GLP-1 can be beneficial in many different diseases characterized by excess inflammation (Hölscher, 2014; Quarta et al., 2017). GLP-1R agonists have been shown to decrease the number of activated microglia in mouse models of diet-induced obesity, stroke, Alzheimer's disease, and Parkinson's disease (Barreto-Vianna et al., 2016; Gao et al., 2014; Kim et al., 2009; McClean et al., 2010; Teramoto et al., 2011; Yun et al., 2018). This study focused only on short-term effects of GLP-1R signaling on diet-induced hypothalamic inflammation and leptin sensitivity. Thus, future studies are needed to address the long-term effects of GLP-1R signaling on diet-induced hypothalamic inflammation and its metabolic consequences. Future studies are also needed to determine the role of astrocytic GLP-1R signaling in modulating these long-term effects and leptin sensitivity.

Previous results suggest that GF mice are more sensitive to leptin compared with CONV-R mice (Schéle et al., 2013). However, these effects could be because of a reduced body weight in GF mice. Our results suggest that leptin-induced pSTAT3 signaling is enhanced in mice lacking a microbiota independent of body weight and circulating leptin levels. In line with previous studies (Shirazi et al., 2013), we show an interaction between hypothalamic leptin and GLP-1 signaling. We demonstrated that Abx treatment in Western diet-fed WT mice, but not in GLP-1R-deficient mice, improved leptin-induced pSTAT3 signaling in the ARC. Previous studies indicate that leptin can stimulate GLP-1 secretion from the intestinal L cells (Anini and Brubaker, 2003). However, short-term administration of leptin did not increase the circulating GLP-1 levels, suggesting that the enhanced leptin-induced pSTAT3 signaling, induced by Abx treatment in this study, is not likely due to leptin-induced GLP-1 secretion.

In concordance with previous results, we found that the *Gcg* expression in the proximal colon was decreased in GF mice after feeding a Western diet (Wichmann et al., 2013). However, in contrast with the colonic *Gcg* expression, the circulating levels of GLP-1 remained elevated in 1- and 4-week Western diet-fed microbiota-depleted mice compared with CONV-R mice, suggesting that either the majority of the circulating GLP-1 does not originate from the proximal colon, the secreted levels may be disconnected from RNA expression, or a longer period of high-fat feeding is necessary to reduce the circulating GLP-1 levels.

The microbial regulation of intestinal GLP-1 secretion is increasingly complex. Colonic depletion of the microbially produced SCFAs, as well as colonic stimulation using SCFAs, increase the circulating GLP-1 levels (Psichas et al., 2015; Wichmann et al., 2013). SCFAs are associated with beneficial metabolic effects (Canfora et al., 2015), and reduced abundance of certain SCFA-producing microbes is associated with metabolic disorders, such as type 2 diabetes (Karlsson et al., 2013; Qin et al., 2012; Wu et al., 2020). Furthermore, mice given a high-fat diet supplemented with SCFAs (i.e., acetate, propionate, or butyrate) exhibit increased energy expenditure and reduced weight gain compared with mice given a comparable high-fat diet without supplementation (den Besten et al., 2015a). Our data, together with previous studies (den Besten et al., 2015a, 2015b), suggest that at least part of this protection against diet-induced obesity is due to GLP-1's effects on leptin sensitivity. Taken together, some of the beneficial effects of SCFAs may indirectly reflect a GLP-1R-mediated reduction in hypothalamic inflammation and improvement in leptin sensitivity.

In conclusion, we show that the gut microbiota can modulate hypothalamic inflammation and leptin sensitivity, findings that require a functional GLP-1R. Thus, an intervention targeting the gut microbiota-GLP-1 axis might be used to modulate this system and reduce the hypothalamic inflammatory response to nutrient excess.

STAR★METHODS

Detailed methods are provided in the online version of this paper and include the following:

- KEY RESOURCES TABLE
- RESOURCE AVAILABILITY

SUPPLEMENTAL INFORMATION

Supplemental information can be found online at https://doi.org/10.1016/j.celrep.2021.109163.

ACKNOWLEDGMENTS

We thank Anita Wichmann, Anna Hallén, Oskar Persson, Per-Olof Bergh, Carina Arvidsson, Louise Helldén, Zakarias Gulic, Caroline Wennberg, and Gabriéla Ryden for technical assistance; Rosie Perkins for comments on the manuscript; and Anna Hallén for help with the artwork. This work was in part supported by grants from the Swedish Research Council, Åke Wiberg Foundation, Magnus Bergvall's Foundation, Wilhelm and Martina Lundgren's foundation, and an International Starting Grant from the Sahlgrenska Academy to L.E.O., as well as grants from the Swedish Research Council, Leducq Foundation, Novo Nordisk Foundation (NNF15OC0016798), Swedish Diabetes Foundation, Swedish Heart-Lung Foundation, Knut and Alice Wallenberg Foundation, and the Swedish state under the agreement between the Swedish government and the county councils, the ALF-agreement (ALFGBG-718101) to F.B. F.B. is a Torsten Söderberg Professor in Medicine and recipient of a European Research Council (ERC) Consolidator Grant (615362-METABASE). D.J.D. is supported by CIHR grant 154321, the Banting and Best Diabetes Centre Novo Nordisk Chair in Incretin Biology, and the Novo Nordisk Foundation-Mt. Sinai Hospital Fund in peptide hormone biology.

AUTHOR CONTRIBUTIONS

Conceptualization, C.N.H., F.B., and L.E.O.; methodology, C.N.H., F.B., and L.E.O.; investigation, C.N.H., L.M.-H., Y.S.L., J.S.-L., A.H.G., and L.E.O.; writing – original draft, C.N.H. and L.E.O.; writing – review & editing, L.M.H., Y.S.L., J.S.-L., A.H.G., R.J.S., D.J.D., and F.B.; funding acquisition, F.B. and L.E.O.; resources, R.J.S. and D.J.D.; supervision, F.B. and L.E.O.

DECLARATION OF INTERESTS

D.J.D. has served as an advisor or consultant or speaker within the past 12 months to Forkhead Biotherapeutics, Intarcia Therapeutics, Kallyope, Eli Lilly, Merck Research Laboratories, Novo Nordisk Inc., and Pfizer Inc. Neither D.J.D. nor his family members hold stock in these companies. GLP-2 is the subject of a patent license agreement between Shire Inc. and the University of Toronto, Toronto General Hospital (UHN), and D.J.D. R.J.S. has research support from Ethicon Endo-Surgery/Johnson & Johnson, Novo Nordisk, Zafgen, Kallyope, Astra Zeneca, and Pfizer. He has been a consultant or part of a Scientific Advisory Board for Ethicon Endo-Surgery/Johnson & Johnson, Novo Nordisk, Janssen/Johnson & Johnson, Sanofi, Kallyope, Scohia, Ironwood Pharma, and GuidePoint Consultants. In addition, R.J.S. holds equity in Zafgen and Redesign Health.

Received: November 5, 2020
Revised: April 6, 2021
Accepted: April 29, 2021
Published: May 25, 2021

REFERENCES

Anini, Y., and Brubaker, P.L. (2003). Role of leptin in the regulation of glucagon-like peptide-1 secretion. Diabetes *52*, 252–259.

Appel, J.R., Ye, S., Tang, F., Sun, D., Zhang, H., Mei, L., and Xiong, W.C. (2018). Increased Microglial Activity, Impaired Adult Hippocampal Neurogenesis, and Depressive-like Behavior in Microglial VPS35-Depleted Mice. J. Neurosci. *38*, 5949–5968.

Bäckhed, F., Ding, H., Wang, T., Hooper, L.V., Koh, G.Y., Nagy, A., Semenkovich, C.F., and Gordon, J.I. (2004). The gut microbiota as an environmental factor that regulates fat storage. Proc. Natl. Acad. Sci. USA *101*, 15718–15723.

Bäckhed, F., Manchester, J.K., Semenkovich, C.F., and Gordon, J.I. (2007). Mechanisms underlying the resistance to diet-induced obesity in germ-free mice. Proc. Natl. Acad. Sci. USA *104*, 979–984.

Barreto-Vianna, A.R., Aguila, M.B., and Mandarim-de-Lacerda, C.A. (2016). Effects of liraglutide in hypothalamic arcuate nucleus of obese mice. Obesity (Silver Spring) *24*, 626–633.

Bates, S.H., Stearns, W.H., Dundon, T.A., Schubert, M., Tso, A.W., Wang, Y., Banks, A.S., Lavery, H.J., Haq, A.K., Maratos-Flier, E., et al. (2003). STAT3 signalling is required for leptin regulation of energy balance but not reproduction. Nature *421*, 856–859.

Baufeld, C., Osterloh, A., Prokop, S., Miller, K.R., and Heppner, F.L. (2016). High-fat diet-induced brain region-specific phenotypic spectrum of CNS resident microglia. Acta Neuropathol. *132*, 361–375.

Canfora, E.E., Jocken, J.W., and Blaak, E.E. (2015). Short-chain fatty acids in control of body weight and insulin sensitivity. Nat. Rev. Endocrinol. *11*, 577–591.

Cani, P.D., Bibiloni, R., Knauf, C., Waget, A., Neyrinck, A.M., Delzenne, N.M., and Burcelin, R. (2008). Changes in gut microbiota control metabolic endotoxemia-induced inflammation in high-fat diet-induced obesity and diabetes in mice. Diabetes *57*, 1470–1481.

Carvajal-Aldaz, D.G., Guice, J.L., Page, R.C., Raggio, A.M., Martin, R.J., Husseneder, C., Durham, H.A., Geaghan, J., Janes, M., Gauthier, T., et al. (2017). Simultaneous delivery of antibiotics neomycin and ampicillin in drinking water inhibits fermentation of resistant starch in rats. Mol. Nutr. Food Res. *61*, 1600609.

Considine, R.V., Sinha, M.K., Heiman, M.L., Kriauciunas, A., Stephens, T.W., Nyce, M.R., Ohannesian, J.P., Marco, C.C., McKee, L.J., Bauer, T.L., et al. (1996). Serum immunoreactive-leptin concentrations in normal-weight and obese humans. N. Engl. J. Med. *334*, 292–295.

den Besten, G., Bleeker, A., Gerding, A., van Eunen, K., Havinga, R., van Dijk, T.H., Oosterveer, M.H., Jonker, J.W., Groen, A.K., Reijngoud, D.J., and Bakker, B.M. (2015a). Short-Chain Fatty Acids Protect Against High-Fat Diet-Induced Obesity via a PPARγ-Dependent Switch From Lipogenesis to Fat Oxidation. Diabetes *64*, 2398–2408.

den Besten, G., Gerding, A., van Dijk, T.H., Ciapaite, J., Bleeker, A., van Eunen, K., Havinga, R., Groen, A.K., Reijngoud, D.J., and Bakker, B.M. (2015b). Protection against the Metabolic Syndrome by Guar Gum-Derived Short-Chain Fatty Acids Depends on Peroxisome Proliferator-Activated Receptor γ and Glucagon-Like Peptide-1. PLoS ONE *10*, e0136364.

Donohoe, D.R., Wali, A., Brylawski, B.P., and Bultman, S.J. (2012). Microbial regulation of glucose metabolism and cell-cycle progression in mammalian colonocytes. PLoS ONE *7*, e46589.

Drucker, D.J. (2007). The role of gut hormones in glucose homeostasis. J. Clin. Invest. *117*, 24–32.

Erny, D., Hrabě de Angelis, A.L., Jaitin, D., Wieghofer, P., Staszewski, O., David, E., Keren-Shaul, H., Mahlakoiv, T., Jakobshagen, K., Buch, T., et al. (2015). Host microbiota constantly control maturation and function of microglia in the CNS. Nat. Neurosci. *18*, 965–977.

Ganat, Y.M., Silbereis, J., Cave, C., Ngu, H., Anderson, G.M., Ohkubo, Y., Ment, L.R., and Vaccarino, F.M. (2006). Early postnatal astroglial cells produce multilineage precursors and neural stem cells in vivo. J. Neurosci. *26*, 8609–8621.

Gao, Y., Ottaway, N., Schriever, S.C., Legutko, B., García-Cáceres, C., de la Fuente, E., Mergen, C., Bour, S., Thaler, J.P., Seeley, R.J., et al. (2014). Hormones and diet, but not body weight, control hypothalamic microglial activity. Glia *62*, 17–25.

Hölscher, C. (2014). Central effects of GLP-1: new opportunities for treatments of neurodegenerative diseases. J. Endocrinol. *221*, T31–T41.

Kanoski, S.E., Ong, Z.Y., Fortin, S.M., Schlessinger, E.S., and Grill, H.J. (2015). Liraglutide, leptin and their combined effects on feeding: additive intake reduction through common intracellular signalling mechanisms. Diabetes Obes. Metab. *17*, 285–293.

Karlsson, F.H., Tremaroli, V., Nookaew, I., Bergström, G., Behre, C.J., Fagerberg, B., Nielsen, J., and Bäckhed, F. (2013). Gut metagenome in European women with normal, impaired and diabetic glucose control. Nature *498*, 99–103.

Kim, S., Moon, M., and Park, S. (2009). Exendin-4 protects dopaminergic neurons by inhibition of microglial activation and matrix metalloproteinase-3 expression in an animal model of Parkinson's disease. J. Endocrinol. *202*, 431–439.

Langlet, F., Levin, B.E., Luquet, S., Mazzone, M., Messina, A., Dunn-Meynell, A.A., Balland, E., Lacombe, A., Mazur, D., Carmeliet, P., et al. (2013). Tanycytic VEGF-A boosts blood-hypothalamus barrier plasticity and access of metabolic signals to the arcuate nucleus in response to fasting. Cell Metab. *17*, 607–617.

Lawrence, T., Willoughby, D.A., and Gilroy, D.W. (2002). Anti-inflammatory lipid mediators and insights into the resolution of inflammation. Nat. Rev. Immunol. *2*, 787–795.

Lee, C.H., Jeon, S.J., Cho, K.S., Moon, E., Sapkota, A., Jun, H.S., Ryu, J.H., and Choi, J.W. (2018). Activation of Glucagon-Like Peptide-1 Receptor Promotes Neuroprotection in Experimental Autoimmune Encephalomyelitis by Reducing Neuroinflammatory Responses. Mol. Neurobiol. *55*, 3007–3020.

McClean, P.L., Gault, V.A., Harriott, P., and Hölscher, C. (2010). Glucagon-like peptide-1 analogues enhance synaptic plasticity in the brain: a link between diabetes and Alzheimer's disease. Eur. J. Pharmacol. *630*, 158–162.

McNeil, N.I. (1984). The contribution of the large intestine to energy supplies in man. Am. J. Clin. Nutr. *39*, 338–342.

Molinaro, A., Caesar, R., Holm, L.M., Tremaroli, V., Cani, P.D., and Bäckhed, F. (2017). Host-microbiota interaction induces bi-phasic inflammation and glucose intolerance in mice. Mol. Metab. *6*, 1371–1380.

Müller, T.D., Finan, B., Bloom, S.R., D'Alessio, D., Drucker, D.J., Flatt, P.R., Fritsche, A., Gribble, F., Grill, H.J., Habener, J.F., et al. (2019). Glucagon-like peptide 1 (GLP-1). Mol. Metab. *30*, 72–130.

Mullier, A., Bouret, S.G., Prevot, V., and Dehouck, B. (2010). Differential distribution of tight junction proteins suggests a role for tanycytes in blood-hypothalamus barrier regulation in the adult mouse brain. J. Comp. Neurol. *518*, 943–962.

Olofsson, L.E., Unger, E.K., Cheung, C.C., and Xu, A.W. (2013). Modulation of AgRP-neuronal function by SOCS3 as an initiating event in diet-induced hypothalamic leptin resistance. Proc. Natl. Acad. Sci. USA *110*, E697–E706.

Pan, W.W., and Myers, M.G., Jr. (2018). Leptin and the maintenance of elevated body weight. Nat. Rev. Neurosci. *19*, 95–105.

Psichas, A., Sleeth, M.L., Murphy, K.G., Brooks, L., Bewick, G.A., Hanyaloglu, A.C., Ghatei, M.A., Bloom, S.R., and Frost, G. (2015). The short chain fatty acid propionate stimulates GLP-1 and PYY secretion via free fatty acid receptor 2 in rodents. Int. J. Obes. *39*, 424–429.

Qin, J., Li, Y., Cai, Z., Li, S., Zhu, J., Zhang, F., Liang, S., Zhang, W., Guan, Y., Shen, D., et al. (2012). A metagenome-wide association study of gut microbiota in type 2 diabetes. Nature *490*, 55–60.

Quarta, C., Clemmensen, C., Zhu, Z., Yang, B., Joseph, S.S., Lutter, D., Yi, C.X., Graf, E., García-Cáceres, C., Legutko, B., et al. (2017). Molecular Integration of Incretin and Glucocorticoid Action Reverses Immunometabolic Dysfunction and Obesity. Cell Metab. *26*, 620–632.e6.

Rüttimann, E.B., Arnold, M., Hillebrand, J.J., Geary, N., and Langhans, W. (2009). Intrameal hepatic portal and intraperitoneal infusions of glucagon-like peptide-1 reduce spontaneous meal size in the rat via different mechanisms. Endocrinology *150*, 1174–1181.

Schéle, E., Grahnemo, L., Anesten, F., Hallén, A., Bäckhed, F., and Jansson, J.O. (2013). The gut microbiota reduces leptin sensitivity and the expression of the obesity-suppressing neuropeptides proglucagon (Gcg) and brain-derived neurotrophic factor (Bdnf) in the central nervous system. Endocrinology *154*, 3643–3651.

Schwartz, M.W., Woods, S.C., Porte, D., Jr., Seeley, R.J., and Baskin, D.G. (2000). Central nervous system control of food intake. Nature *404*, 661–671.

Scrocchi, L.A., Brown, T.J., MaClusky, N., Brubaker, P.L., Auerbach, A.B., Joyner, A.L., and Drucker, D.J. (1996). Glucose intolerance but normal satiety in mice with a null mutation in the glucagon-like peptide 1 receptor gene. Nat. Med. *2*, 1254–1258.

Shirazi, R., Palsdottir, V., Collander, J., Anesten, F., Vogel, H., Langlet, F., Jaschke, A., Schürmann, A., Prévot, V., Shao, R., et al. (2013). Glucagon-like peptide 1 receptor induced suppression of food intake, and body weight is mediated by central IL-1 and IL-6. Proc. Natl. Acad. Sci. USA *110*, 16199–16204.

Sokol, H., Pigneur, B., Watterlot, L., Lakhdari, O., Bermúdez-Humarán, L.G., Gratadoux, J.J., Blugeon, S., Bridonneau, C., Furet, J.P., Corthier, G., et al. (2008). Faecalibacterium prausnitzii is an anti-inflammatory commensal bacterium identified by gut microbiota analysis of Crohn disease patients. Proc. Natl. Acad. Sci. USA *105*, 16731–16736.

Sonnenburg, J.L., and Bäckhed, F. (2016). Diet-microbiota interactions as moderators of human metabolism. Nature *535*, 56–64.

Teramoto, S., Miyamoto, N., Yatomi, K., Tanaka, Y., Oishi, H., Arai, H., Hattori, N., and Urabe, T. (2011). Exendin-4, a glucagon-like peptide-1 receptor agonist, provides neuroprotection in mice transient focal cerebral ischemia. J. Cereb. Blood Flow Metab. *31*, 1696–1705.

Thaler, J.P., Yi, C.X., Schur, E.A., Guyenet, S.J., Hwang, B.H., Dietrich, M.O., Zhao, X., Sarruf, D.A., Izgur, V., Maravilla, K.R., et al. (2012). Obesity is associated with hypothalamic injury in rodents and humans. J. Clin. Invest. *122*, 153–162.

Thaler, J.P., Guyenet, S.J., Dorfman, M.D., Wisse, B.E., and Schwartz, M.W. (2013). Hypothalamic inflammation: marker or mechanism of obesity pathogenesis? Diabetes *62*, 2629–2634.

Timper, K., Del Río-Martín, A., Cremer, A.L., Bremser, S., Alber, J., Giavalisco, P., Varela, L., Heilinger, C., Nolte, H., Trifunovic, A., et al. (2020). GLP-1 Receptor Signaling in Astrocytes Regulates Fatty Acid Oxidation, Mitochondrial Integrity, and Function. Cell Metab. *31*, 1189–1205.e13.

Valdearcos, M., Robblee, M.M., Benjamin, D.I., Nomura, D.K., Xu, A.W., and Koliwad, S.K. (2014). Microglia dictate the impact of saturated fat consumption on hypothalamic inflammation and neuronal function. Cell Rep. *9*, 2124–2138.

Wang, S., Huang, M., You, X., Zhao, J., Chen, L., Wang, L., Luo, Y., and Chen, Y. (2018). Gut microbiota mediates the anti-obesity effect of calorie restriction in mice. Sci. Rep. *8*, 13037.

Wichmann, A., Allahyar, A., Greiner, T.U., Plovier, H., Lundén, G.O., Larsson, T., Drucker, D.J., Delzenne, N.M., Cani, P.D., and Bäckhed, F. (2013). Microbial modulation of energy availability in the colon regulates intestinal transit. Cell Host Microbe *14*, 582–590.

Wilson-Pérez, H.E., Chambers, A.P., Ryan, K.K., Li, B., Sandoval, D.A., Stoffers, D., Drucker, D.J., Pérez-Tilve, D., and Seeley, R.J. (2013). Vertical sleeve gastrectomy is effective in two genetic mouse models of glucagon-like Peptide 1 receptor deficiency. Diabetes *62*, 2380–2385.

Wu, H., Tremaroli, V., Schmidt, C., Lundqvist, A., Olsson, L.M., Krämer, M., Gummesson, A., Perkins, R., Bergström, G., and Bäckhed, F. (2020). The Gut Microbiota in Prediabetes and Diabetes: A Population-Based Cross-Sectional Study. Cell Metab. *32*, 379–390.e3.

Yulyaningsih, E., Rudenko, I.A., Valdearcos, M., Dahlén, E., Vagena, E., Chan, A., Alvarez-Buylla, A., Vaisse, C., Koliwad, S.K., and Xu, A.W. (2017). Acute Lesioning and Rapid Repair of Hypothalamic Neurons outside the Blood-Brain Barrier. Cell Rep. *19*, 2257–2271.

Yun, S.P., Kam, T.I., Panicker, N., Kim, S., Oh, Y., Park, J.S., Kwon, S.H., Park, Y.J., Karuppagounder, S.S., Park, H., et al. (2018). Block of A1 astrocyte conversion by microglia is neuroprotective in models of Parkinson's disease. Nat. Med. *24*, 931–938.

Zarrinpar, A., Chaix, A., Xu, Z.Z., Chang, M.W., Marotz, C.A., Saghatelian, A., Knight, R., and Panda, S. (2018). Antibiotic-induced microbiome depletion alters metabolic homeostasis by affecting gut signaling and colonic metabolism. Nat. Commun. *9*, 2872.

STAR★METHODS

KEY RESOURCES TABLE

REAGENT or RESOURCE	SOURCE	IDENTIFIER
Antibodies		
GFAP antibody, goat	Abcam	RRID AB_880202: ab53554
Iba1 antibody, rabbit	Wako	RRID AB_839504: Cat# 019-19741
Cfos antibody, rabbit	Santa Cruz	RRID AB_2106783: Cat# sc-52 (discontinued 2016)
Phospho-stat-3 (tyr705) antibody	Cell signaling	RRID AB_331586: Cat# 9131
GLP-1R antibody	Abcam	RRID AB_2864762: Cat# 218532
AlexaFluor donkey anti-goat IgG 488	Thermo Fisher Scientific	RRID AB_2866497: Cat# a32814TR
AlexaFluor donkey anti-goat IgG 594	Thermo Fisher Scientific	RRID AB_2534105: Cat# A-11058
AlexaFluor donkey anti-rabbit IgG 594	Thermo Fisher Scientific	RRID AB_141637: Cat# a-21207
AlexaFluor donkey anti-rabbit IgG 488	Thermo Fisher Scientific	RRID AB_2535792: Cat# a-21206
Hoechst 33342	Thermo Fisher Scientific	Cat# H1399
Chemicals, peptides, and recombinant proteins		
QIAzol Lysis Reagent	QIAGEN	CAS N/A: Cat# 79306
SYBR Green Master Mix Buffer	Bio-Rad	CAS N/A: Cat# 1708887
DPPIV-inhibitor	Sigma	CAS: N/A: Cat# DPP4-010
Aprotinin	Merck	CAS: 9087-70-1: Cat# 616399 /A6279
Leptin	Peprotech	CAS: N/A: Cat# 450-31
Exendin (9-39)	Bachem	CAS: 133514-43-9: Cat# H-8740
Exendin 4	Sigma	CAS: 141758-74-9: Cat# E7144
Etanercept	Merck	CAS: 185243-69-0: Cat# Y0002042
AF12198	Tocris	CAS: 185413-30-3: Cat# 1793
Tamoxifen	Merck	CAS: 10540-29-1: Cat# T5648
ampicillin	Merck	CAS: 69-52-3: Cat# A9518
neomycin	Merck	CAS: 1405-10-3: Cat# N6386
Critical commercial assays		
Mouse Metabolic Kit	Meso Scale Discovery	RRID N/A: Cat# K15124C
Total GLP-1 (ver.2) Kit	Meso Scale Discovery	RRID AB_2801383: Cat# K150JVC
High Capacity cDNA Reverse Transcription Kit	Applied Biosystems, Thermo Fisher Scientific	RRID N/A: Cat# 4368813
RNeasy mini Kit	QIAGEN	RRID N/A: Cat# 74106
Experimental models: Organisms/strains		
C57BL/6J	N/A	N/A
Cx3cr1CreER: B6.129P2(Cg)-Cx3cr1tm2.1(cre/ERT2)Litt/WganJ	The Jackson Laboratory	IMSR Cat# JAX:021160, RRID:IMSR_JAX:021160
GCE: B6.Cg-Tg(GFAP-cre/ERT2)505Fmv/J	The Jackson Laboratory	IMSR Cat# JAX:012849, RRID:IMSR_JAX:012849
ROSA mTmG mice: B6.129(Cg)-Gt(ROSA)26Sortm4(ACTB-tdTomato,-EGFP)Luo/J	The Jackson Laboratory	IMSR Cat# JAX:007676, RRID:IMSR_JAX:007676
Glp-1r−/−	Dr. Daniel Drucker	N/A
Glp1rflox/flox	Dr. Randy Seeley	N/A
Oligonucleotides		
Il1b-F GGGCCTCAAAGGAAAGAATC	This paper	N/A
Il1b-R TACCAGTTGGGGAACTCTGC	This paper	N/A
Il6-F TCCTACCCCAATTTCCAATG	Molinaro et al., 2017	N/A

(*Continued on next page*)

Continued		
REAGENT or RESOURCE	SOURCE	IDENTIFIER
Il6-R GGTTTGCCGAGTAGATCTCAA	Molinaro et al., 2017	N/A
TNFa-F CCAGACCCTCACACTCA	Molinaro et al., 2017	N/A
TNFa-R CACTTGGTGGTTTGCTACGAC	Molinaro et al., 2017	N/A
L32-F CCTCTGGTGAAGCCCAAGATC	Molinaro et al., 2017	N/A
L32-R TCTGGGTTTCCGCCAGTTT	Molinaro et al., 2017	N/A
Software and algorithms		
GraphPad Prism 7/8/9	GraphPad Software	Latest version 8.3.0
ImageJ		https://imagej.nih.gov/ij/
Other		
Irradiated Western Diet, 40% kcal fat	Envigo	Cat# TD09683
chow diet (Autoclaved mouse breeder diet)	Labdiet	#5021
Alzet Osmotic Minipumps	ALZET, model 2002, Agnthos	Cat# 0000296
CFX96 Real-Time System	Bio-Rad	
PhenoMaster	TSE Systems	
MRI	EchoMRI	

RESOURCE AVAILABILITY

Lead contact

For further information and requests for resources and reagents please reach out to the lead contact, Louise Olofsson (Louise.Olofsson@wlab.gu.se).

Materials availability

This study did not generate new unique reagents.

Data and Code Availability

This study did not generate or use any datasets or code.

EXPERIMENTAL MODEL AND SUBJECT DETAILS

Mice

All experiments were approved by the ethical committee at the University of Gothenburg. Mice were housed in a room with a 12-h light-dark cycle with free access to water and food. C57BL/6J male mice (10-13 weeks old) were used in the experiments unless otherwise stated. GF mice were maintained in flexible film isolators and the GF status was monitored regularly by PCR for bacterial 16S ribosomal RNA. Mice lacking GLP-1R have previously been described and characterized (Scrocchi et al., 1996). Mice expressing tamoxifen-induced Cre under the *Cx3cr1* promoter (B6.129P2(Cg)-*Cx3cr1*$^{tm2.1(cre/ERT2)Litt}$/WganJ) or the *Gfap* promoter (B6.Cg-Tg(GFAP-cre/ERT2)505Fmv/J) were purchased from The Jackson Laboratory (Bar Harbor, ME) and have previously been characterized (Appel et al., 2018; Ganat et al., 2006). These tamoxifen-inducible Cre mice were bred with *Glp1r*$^{flox/flox}$ mice (Wilson-Pérez et al., 2013) or ROSA mTmG reporter mice (B6.129(Cg)-*Gt(ROSA)26Sor*$^{tm4(ACTB-tdTomato,-EGFP)Luo}$/J). To induce Cre expression, mutant mice were injected with tamoxifen (100 mg/kg; T5648, Merck, Darmstadt, Germany) intraperitoneal (i.p.) once a day for five consecutive days. Tamoxifen was dissolved in a solution containing 5% ethanol and 95% peanut oil (Merck). Controls were injected with either tamoxifen or vehicle. Since there was no difference in gliosis between the tamoxifen and vehicle injected mice, these two groups were combined. Mice were either fed autoclaved chow diet (Labdiet, St. Louis, MO) or irradiated Western diet (40% kcal fat, TD09683, Envigo, Huntingdon, UK). Western diet was given for 2 days, 1 week or 4 weeks as indicated. Table S1 gives a detailed overview of the animal experiments performed.

METHOD DETAILS

Antibiotic treatment

Mice were treated with antibiotics according to a protocol previously described (Cani et al., 2008). Briefly, 1 g/l ampicillin (A9518, Merck) and 0.5 g/l neomycin (N6386, Merck) were added to the drinking water in light protected bottles. New solutions were prepared

every second day. Depletion of microbes after antibiotic treatment was confirmed (Figures S1E–S1K). In experiments when mice were given both antibiotic treatment and a Western diet, the antibiotic treatment started three days before changing to a Western diet.

Colony forming units counts

LyBHI was prepared as described previously (Sokol et al., 2008). Cecum content was dissolved in LyBHI broth and dilution series were plated on LyBHI Agar plates (20 g agar/l). Plates were incubated overnight under anaerobe (Coy chamber Laboratory products Inc., filled with 85% N_2, 10% CO_2 and 5% H_2, incubator at 37°C,) or aerobe conditions (incubator at 30°C), and the number of colony forming units was determined.

Bacterial staining

Cecum content was dissolved in LyBHI, incubated overnight under anaerobe conditions as described above, and stained for gram-negative bacteria. Broth were placed on microscope slides and dried. Slides were then incubated for 20 s in 0.5% Crystal Violet, washed with MilliQ water, incubated for 20 s in 0.5% iodine solution, washed with 99.5% EtOH, incubated for 20 s with 0.5% Safranin, washed with MilliQ water and dried. Pictures were taken using a Zeiss Microscope (Zeiss, Oberkochen, Germany).

SCFA measurements

SCFA were measured using GC-MS as described previously (Wichmann et al., 2013). Briefly, approximately 100 mg of cecal content was mixed with internal standards, added to glass vials and freeze-dried. Samples were acidified with HCl, and SCFAs were extracted with two rounds of diethyl ether extraction. The organic supernatant was collected, the derivatization agent N-tert-butyldimethylsilyl-N-methyltrifluoroace-tamide (Merck) was added, and samples were incubated overnight. SCFAs were quantified with a gas chromatograph (Agilent 7890A, Agilent Technologies, Santa Clara, CA) coupled to a mass spectrometer (Agilent 5975C, Agilent Technologies).

Administration of agonist and antagonists

For Exendin (9-39) administration, 10- to 11-week-old C57BL/6J mice maintained on a chow diet (Labdiet) were lightly anaesthetized with isoflurane and ALZET osmotic minipumps (ALZET model 2002, Durect, Cupertino, CA) were implanted subcutaneously. The pumps delivered Exendin (9-39) (Bachem, Bubendorf, Switzerland), a GLP-1R antagonist, at a rate of 50 nmol/kg/day or vehicle (0.9% saline) for two weeks. Three days after the osmotic minipump implantation, two groups of CONV-R mice received antibiotic treatment in the drinking water *ad libitum*. Fresh antibiotics were prepared every other day until the end of the experiment. Six days after the osmotic minipump implantation, chow diet was replaced with irradiated Western diet for one week.

For Ex4 administration, chow-fed WT and *Gfap-Glp1r* $^{-/-}$ female mice were fasted for 12 hours before being killed. Ex4 (10 μg/kg) or vehicle was injected 2 hours before the mice were perfused with PFA.

For AF12198 and Etanercept administration, 10- to 12-weeks-old C57BL/6J mice were given a Western diet for one week while injected with 0.5 mg/kg AF12198 (1793, Tocris. Bristol, UK) or 1.5 mg/kg Etanercept (Y0002042, Merck) once a day for five consecutive days starting at the day of diet switch. Since the ARC has an incomplete blood-brain barrier and cells in this brain region readily sense substances in the blood (Olofsson et al., 2013), we administrated AF12198 and Etanercept by i.p. injections.

Immunofluorescence

Mice were perfused with 4% (wt/vol) paraformaldehyde (PFA) in PBS. Brains were dissected, postfixed in 4% PFA and transferred to 30% (wt/vol) sucrose in PBS overnight at 4°C. Part of the brain, containing the hypothalamus, was embedded in OCT (Histolab, Gothenburg, Sweden), frozen and kept in −80°C until sectioned. Brains were sectioned in 10 μm thick coronal sections using a cryostat. For staining of Iba1 and GFAP, sections containing the ARC were incubated sequentially for 10 min each in 0.3% (wt/vol) glycine solution and 0.3% (wt/vol) SDS solution. Sections were blocked in 10% donkey serum for 1 h at room temperature, incubated with primary antibodies against Iba1 (dilution 1:500, 019-19741, Wako Pure Chemicals, Richmond, VA) or GFAP (dilution 1:500, ab53554, Abcam, Cambridge, UK) overnight at 4°C, washed in PBS-tween, and incubated with secondary donkey anti-goat or donkey anti-rabbit antibodies (AlexaFluor, Invitrogen, Waltham, MA) for 1 h at room temperature. For c-*fos* and GFAP co-staining as well as pSTAT3 staining, sections containing the ARC were incubated sequentially for 10 min each in 1% NaOH/1% H_2O_2, 0.3% (wt/vol) glycine and 0.3% (wt/vol) SDS. Sections were blocked in 10% donkey serum for 1 h at room temperature, incubated with primary antibodies against c-*fos* (dilution 1:500, sc-52, Santa Cruz Biotechnology, Dallas, TX), GFAP (dilution 1:500, 13-0300, Thermo Fisher Scientific, Waltham, MA) or pSTAT3 (dilution 1:200, 9131, Cell signaling Technology, Danvers, MA) overnight at 4°C, washed in PBS-tween, and incubated with a secondary donkey anti-rat or donkey anti-rabbit antibody (AlexaFluor, Invitrogen) for 1 h. For GLP-1R and GFAP co-staining, hypothalamic sections were washed in PBS-tween, and incubated for 1 hour at room temperature with blocking solution (2% BSA, 0.1% Triton-X). Sections were incubated with primary antibodies against GLP-1R (dilution 1:500, ab218532, Abcam) and GFAP (dilution 1:500, ab53554, Abcam) overnight at 4°C, washed in PBS-tween and incubated with secondary donkey-anti-rabbit and donkey-anti-goat antibodies (AlexaFluor, Invitrogen). Hoechst solution (dilution 1:10000, H1399, Thermo Fisher Scientific) was used to visualize cell nuclei. Fluorescence images were captured using Zeiss Axioplan 2 imaging system equipped with an AxioCam digital camera HRc using the program Axio Vision 4.8.2.0 (Zeiss). The positive cells in the ARC (Bregma −2.15 to −2.03) were counted blinded and expressed as an average per coronal section (10 μm thick).

GLP-1, leptin and insulin measurements

Mice were fasted for 4 h before plasma collection unless otherwise stated. During the plasma collection, which occurred during the afternoon, DPP-4 inhibitor (DPP4-010, Merck) and Aprotinin (616399-100KU, Merck) were added to both the syringes and the EDTA-containing plasma collection tubes (Sarstedt, Nümbrecht, Germany). Plasma GLP-1 from vena cava or vena porta was measured using Active GLP-1 (ver. 2) Assay Kit (Meso Scale Discovery; Rockville, MD) according to the manufacture's recommendation. Leptin and insulin were measured in plasma using the mouse metabolic kit (Meso Scale Discovery) according to the manufacture's recommendation.

Gene expression analysis

Food was removed from the cages in the morning and tissues were harvested from the mice after a 4-h-fast. RNA was isolated using QIAzol reagent (QIAGEN, Hilden, Germany) and RNeasy mini kit with DNase I treatment (QIAGEN). The samples were homogenized using 5 mm steel beads and a TissueLyser (QIAGEN). RNA (0.5 μg) was reverse transcribed to cDNA using the High Capacity cDNA Reverse Transcription Kit (Applied Biosystems, Waltham, MA) according to the manufacturer's manual. 25 μL qRT-PCR reactions were prepared containing 1 × SYBR Green Master Mix buffer (Bio-Rad, Hercules, CA) and 900 nM specific primers targeting the gene of interest or 300 nM directed against the reference gene L32. Primer sequences for *Tnfa*, *Il6* and *L32* has previously been described (Molinaro et al., 2017). The primer sequences for *Il1b* were GGGCCTCAAAGGAAAGAATC and TACCAGTTGGGGA ACTCTGC. The mRNA levels were analyzed using the CFX96 Real-Time System (Bio-Rad, Hercules, CA). *Il1b*, *Tnfa* and *Il6* gene expression were normalized to the expression level of the ribosomal protein L32 using the $\Delta\Delta C_T$ method and analyzed by calculating the relative gene expression.

Body composition analysis and leptin sensitivity test

Lean and fat mass were determined using MRI (EchoMRI, Houston, TX) according to the manufacturer's recommendation. Mice were i.p. injected with either leptin (3 mg/kg, PeproTech, Rocky Hill, NJ) or vehicle 45 min before being perfused with PBS followed by PFA. The number of pSTAT3-positive cells in the ARC was determined in response to leptin injection. To determine leptin's anorexic effects, food intake was analyzed in metabolic cages (PhenoMaster, TSE Systems, Bad Homburg, Germany). The mice were single housed for at least 2 days before transferring them to the metabolic cages, and allowed an additional 24 h to acclimatize to the new cage before taking measurements. The mice were injected with saline or leptin (3 mg/kg) just before the dark cycle started and the 24-hour food intake was measured in mice with free access to water and Western diet. Each mouse served as its own control and food intake was expressed as percent food intake after leptin injection compared to after saline injection within the same mouse.

QUANTIFICATION AND STATISTICAL ANALYSIS

Statistical analysis

Data are presented as mean ± SEM. Each data point in the figures represent data from one mouse, and shows the mean of at least two replicates for all data except body weight, cecum weight and SCFA analyses. Statistical differences were tested with two-sided Mann-Whitney test, or a Kruskal-Wallis test with Dunn's Multiple Comparison Post-Test as indicated in the figure legends. Statistical analysis was performed using GraphPad Prism 7.

Cell Reports, Volume *35*

Supplemental information

The gut microbiota regulates hypothalamic inflammation and leptin sensitivity in Western diet-fed mice via a GLP-1R-dependent mechanism

Christina N. Heiss, Louise Mannerås-Holm, Ying Shiuan Lee, Julia Serrano-Lobo, Anna Håkansson Gladh, Randy J. Seeley, Daniel J. Drucker, Fredrik Bäckhed, and Louise E. Olofsson

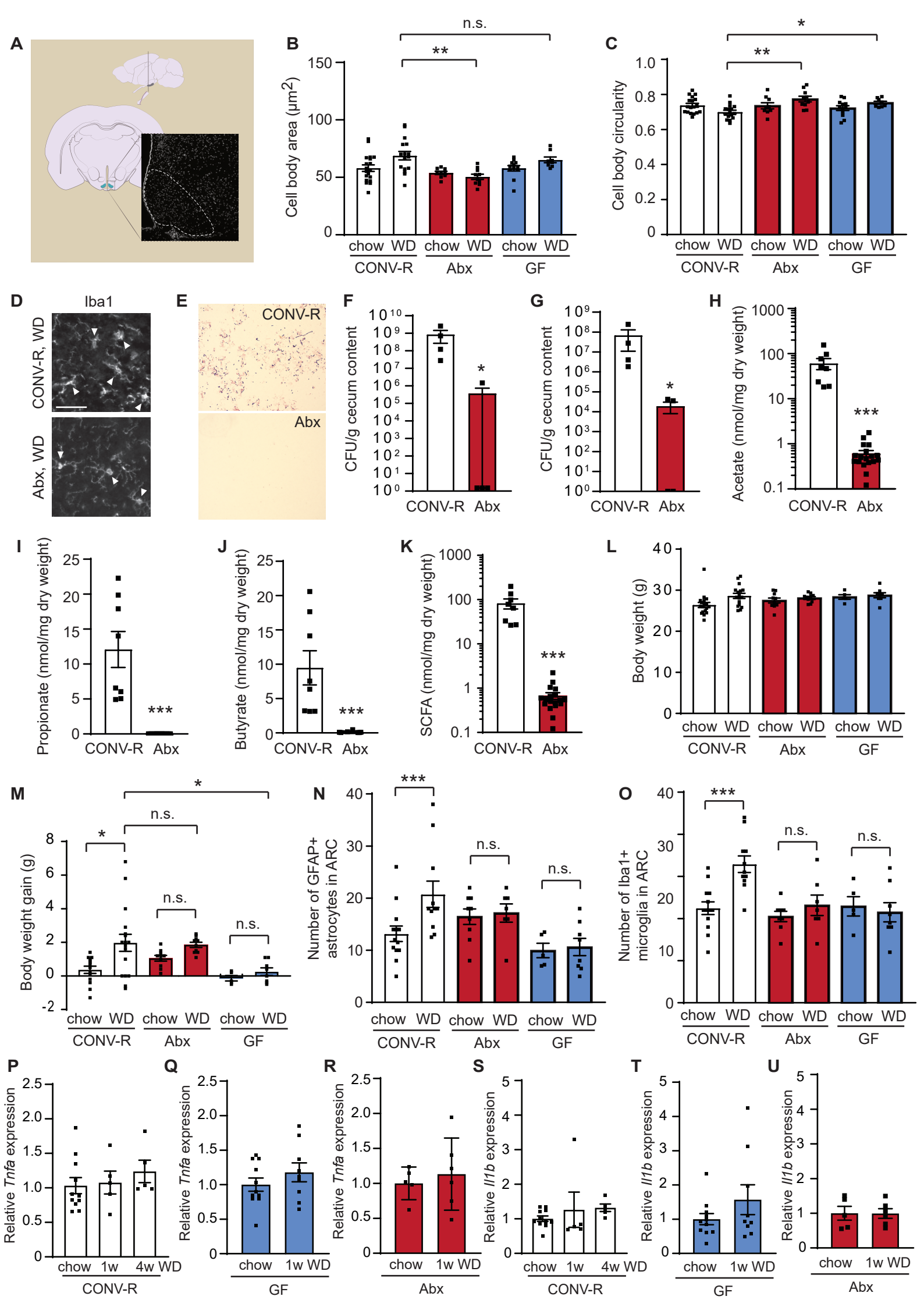
A
B
Cell body area (μm2)
n.s.
**
chow WD chow WD chow WD
CONV-R Abx GF
C
Cell body circularity
*
**
D
Iba1
CONV-R, WD
Abx, WD
E
CONV-R
Abx
F
CFU/g cecum content
CONV-R Abx
G
CFU/g cecum content
CONV-R Abx
H
Acetate (nmol/mg dry weight)
***
CONV-R Abx
I
Propionate (nmol/mg dry weight)
***
CONV-R Abx
J
Butyrate (nmol/mg dry weight)
***
CONV-R Abx
K
SCFA (nmol/mg dry weight)
***
CONV-R Abx
L
Body weight (g)
chow WD chow WD chow WD
CONV-R Abx GF
M
Body weight gain (g)
*
n.s.
*
n.s.
n.s.
chow WD chow WD chow WD
CONV-R Abx GF
N
Number of GFAP+ astrocytes in ARC
***
n.s.
n.s.
chow WD chow WD chow WD
CONV-R Abx GF
O
Number of Iba1+ microglia in ARC
***
n.s.
n.s.
chow WD chow WD chow WD
CONV-R Abx GF
P
Relative Tnfa expression
chow 1w 4w WD
CONV-R
Q
Relative Tnfa expression
chow 1w WD
GF
R
Relative Tnfa expression
chow 1w WD
Abx
S
Relative Il1b expression
chow 1w 4w WD
CONV-R
T
Relative Il1b expression
chow 1w WD
GF
U
Relative Il1b expression
chow 1w WD
Abx

Figure S1. Mice lacking a microbiota are protected from diet-induced hypothalamic inflammation. Related to Figure 1.

Position of the arcuate nucleus in the brain (A). Figure shows sagittal and coronal views of the brain, as well as Hoechst nuclear staining in hypothalamus (inserted). Arcuate nucleus is marked by a dashed white line. CONV-R, GF and antibiotic-treated mice were fed a chow or a Western diet for one week. Hypothalamic Iba1-positive microglia morphology was analyzed (B-D). Scale bar: 25 μm. Each data point represents the mean cell body area and circularity of all the Iba1-positive microglia from one mouse detected in the arcuate nucleus from 10-μm thick hypothalamic section. n=8-18 mice per group. Depletion of the gut microbiota after antibiotic treatment was confirmed by growing cecum content from CONV-R and antibiotic-treated mice under anaerobe (E-F) or aerobe conditions (G). n=4 mice per group. SCFAs were analyzed in cecum from CONV-R and antibiotic-treated mice (H-K). Panel K shows the sum of acetate, propionate and butyrate levels. n=8-18 mice per group. Body weight and weight gain were determined in chow-fed and 1-week Western diet-fed CONV-R, antibiotic-treated and GF mice (L-M). The number of GFAP-positive astrocytes (N) and Iba1-positive microglia (O) in the hypothalamic arcuate nucleus was determined in weight gain-matched mice. n=5-13 mice per group. Hypothalamic *Tnfα* (P-R) and *Il1b* (S-U) gene expression were analyzed in CONV-R, GF and antibiotic-treated mice given a chow diet or a Western diet. Each data point in the graph represent data from one mouse, and shows the mean of two replicates. n=5-11 mice per group. All graphs show mean ± SEM. *, $P<0.05$, **, $P<0.01$ and ***, $P<0.001$ as determined by Kruskal-Wallis Test in B-C, L-M, P and S or by Mann-Whitney rank test in F-K, N-O, Q-R and T-U. CONV-R, conventionally raised mice; GF, germ-free; Abx, antibiotics.

A

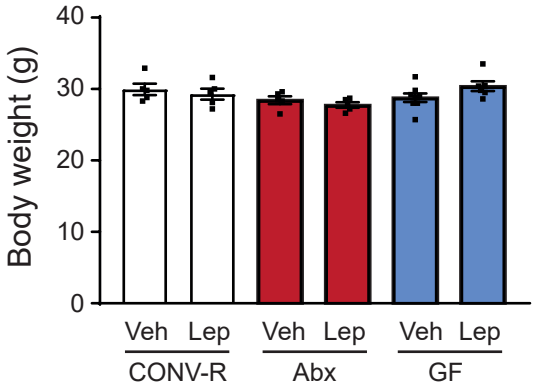
Body weight (g)
40
30
20
10
0
Veh
Lep
Veh
Lep
Veh
Lep
CONV-R
Abx
GF

B

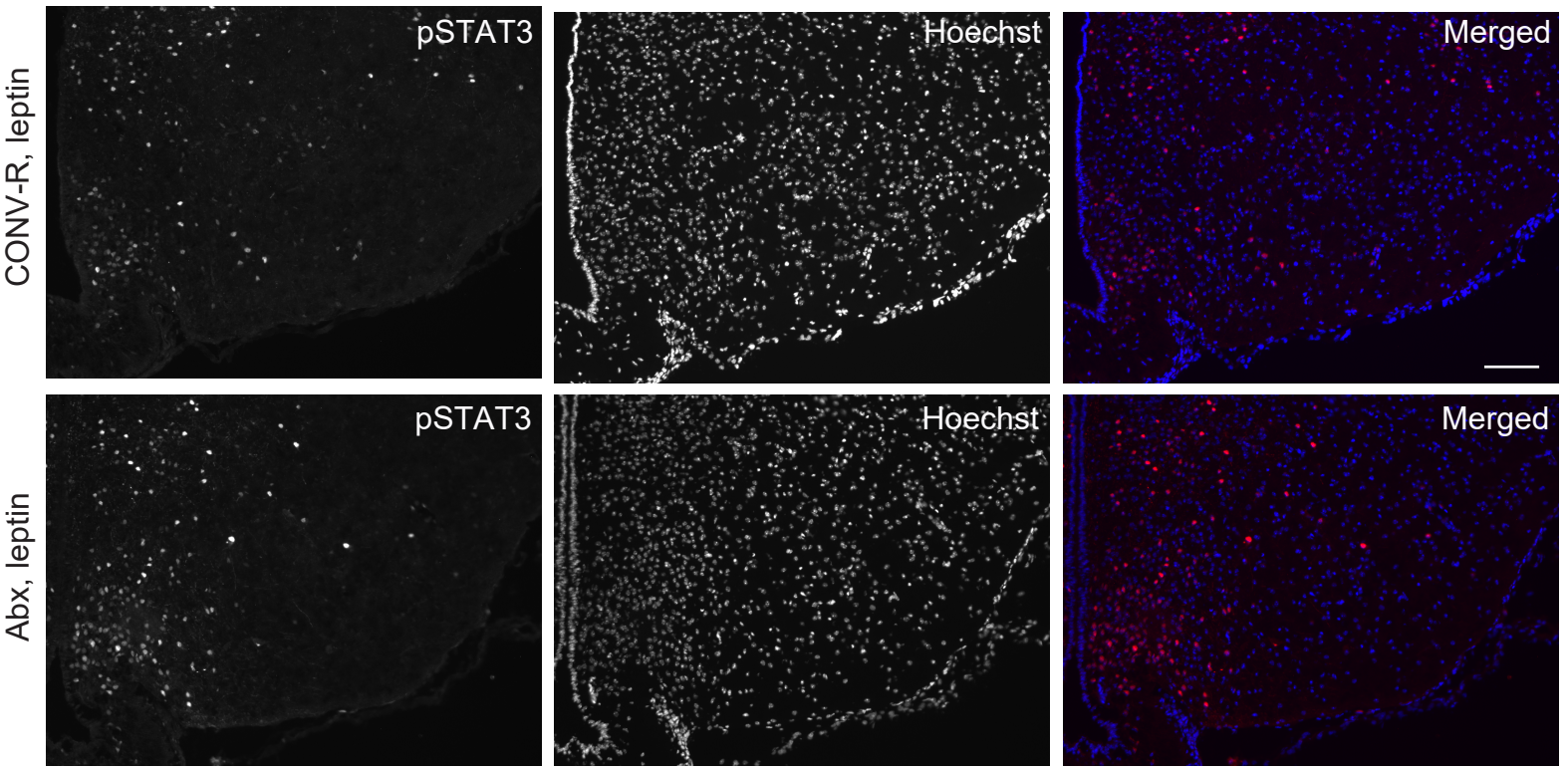
CONV-R, leptin
pSTAT3
Hoechst
Merged
Abx, leptin
pSTAT3
Hoechst
Merged

Figure S2. Microbiota deprivation enhances pSTAT3 signaling upon leptin injection. Related to Figure 2.

CONV-R, antibiotic-treated and GF mice were fed a Western diet for one week and injected with either vehicle or leptin (3 mg/kg) 45 minutes before perfusion. Body weight was measured at the end of the experiment (A). n=4-8 mice per group. Graph shows mean ± SEM. Differences between the groups were tested using Kruskal-Wallis. Representative pictures of pSTAT3 staining in the ARC upon leptin injection in CONV-R and antibiotic-treated mice fed a Western diet for one week (B). Scale bar: 100 μm. CONV-R, conventionally raised mice; GF, germ-free; Abx, antibiotics; Veh, vehicle; Lep, leptin.

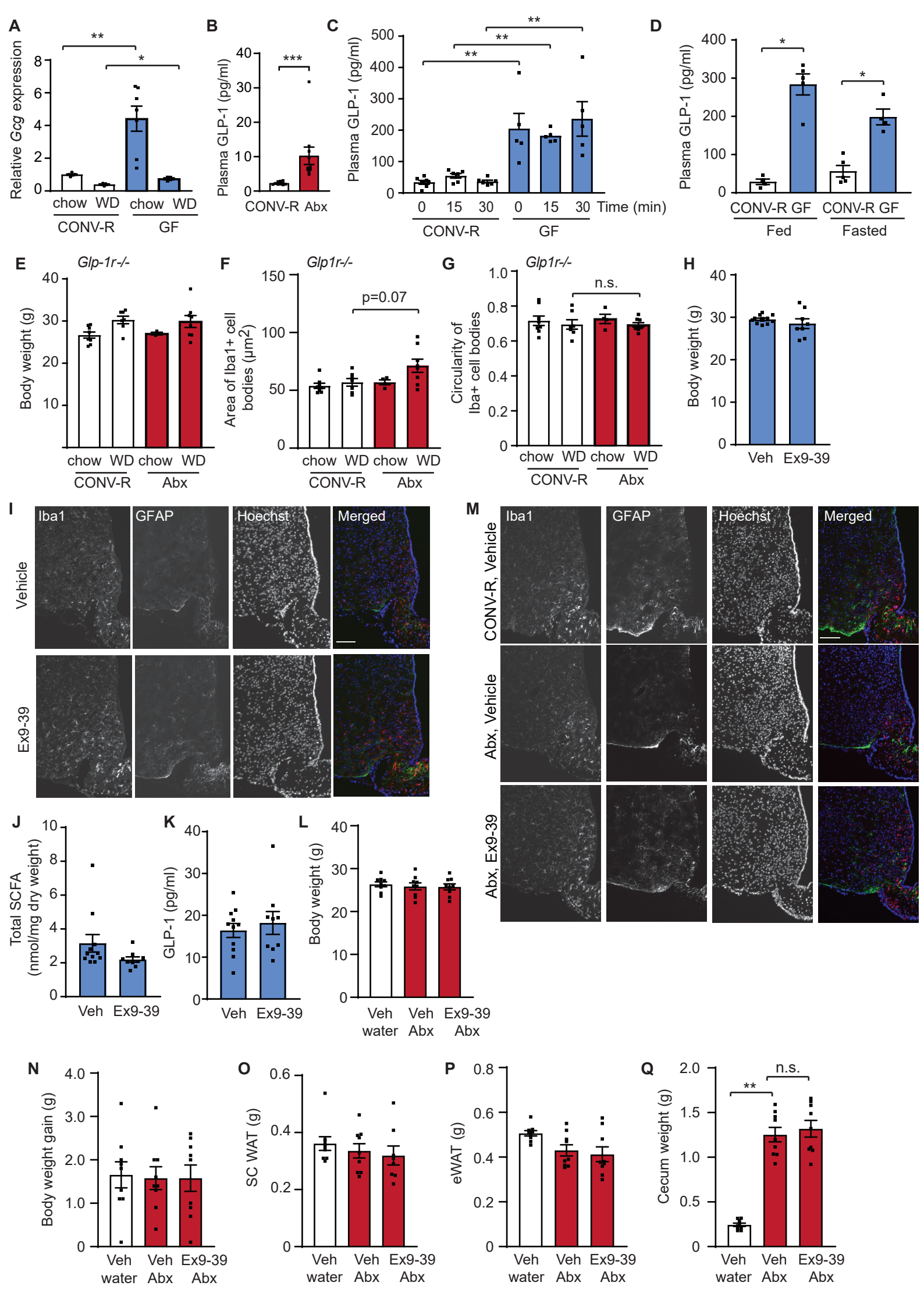
A
Relative Gcg expression
chow WD chow WD
CONV-R GF
B
Plasma GLP-1 (pg/ml)
CONV-R Abx
C
Plasma GLP-1 (pg/ml)
0 15 30 0 15 30 Time (min)
CONV-R GF
D
Plasma GLP-1 (pg/ml)
CONV-R GF CONV-R GF
Fed Fasted
E
Glp-1r-/-
Body weight (g)
chow WD chow WD
CONV-R Abx
F
Glp1r-/-
Area of Iba1+ cell bodies (µm2)
p=0.07
chow WD chow WD
CONV-R Abx
G
Glp1r-/-
Circularity of Iba+ cell bodies
n.s.
chow WD chow WD
CONV-R Abx
H
Body weight (g)
Veh Ex9-39
I
Iba1
GFAP
Hoechst
Merged
Vehicle
Ex9-39
M
Iba1
GFAP
Hoechst
Merged
CONV-R, Vehicle
Abx, Vehicle
Abx, Ex9-39
J
Total SCFA (nmol/mg dry weight)
Veh Ex9-39
K
GLP-1 (pg/ml)
Veh Ex9-39
L
Body weight (g)
Veh water Veh Abx Ex9-39 Abx
N
Body weight gain (g)
Veh water Veh Abx Ex9-39 Abx
O
SC WAT (g)
Veh water Veh Abx Ex9-39 Abx
P
eWAT (g)
Veh water Veh Abx Ex9-39 Abx
Q
Cecum weight (g)
n.s.
Veh water Veh Abx Ex9-39 Abx

Figure S3. Functional GLP-1 receptor signaling is required for the protection against diet-induced hypothalamic inflammation and the improved leptin sensitivity in mice with depleted gut microbiota. Related to Figure 3.

(A) Colonic *Gcg* expression in CONV-R and GF Swiss Webster mice fed chow or Western diet. n= 4-7 per group. Each data point in the graph represents data from one mouse, and shows the mean of two measurements. (B) Plasma GLP-1 in CONV-R and antibiotic-treated mice after 4 weeks of Western diet feeding. n= 10 mice per group. (C) Plasma GLP-1 before and 15 and 30 minutes after an oral glucose challenge (3g D-glucose/kg body weight). n= 5-7 mice per group. (D) Plasma GLP-1 levels in fed and fasted CONV-R and GF mice. n= 4-5 mice per group. All plasma GLP-1 levels were measured in duplicates. (E) Body weight in chow- and Western diet-fed CONV-R and antibiotic-treated GLP-1R-deficient mice (n=4-8 per group). Microglia cell body area (F) and circularity (G) in CONV-R and antibiotic-treated GLP-1R-deficient mice. Each data point represents the mean cell body area and circularity of all the Iba1-positive microglia from one mouse detected in the arcuate nucleus from 10-µm thick hypothalamic section (n=4-9 per group). (H-K) Osmotic pumps, that delivered vehicle or Ex9-39 (50 nmol/kg/day), were implanted subcutaneously in GF mice. n=7-9 mice per group. Body weight was measured at the end of the experiment (H). Representative pictures of Iba1 and GFAP staining in vehicle and Ex9-39 administrated mice (I). Scale bar: 100 µm. Total SCFA (J) and circulating GLP-1 levels (K) were determined at the end of the experiment. Panel K shows the mean of two measurements. (L-Q) Osmotic pumps, that delivered vehicle or Ex9-39 (50 nmol/kg/day), were implanted subcutaneously in CONV-R mice. Three days after surgery, mice were treated with or without antibiotics in the drinking water. Six days after surgery, the mice were switched from a chow to a Western diet. Mice were fed a Western diet for one week, until the end of the experiment. n=8-9 per group. Body weight was measured at the end of the experiment (L). Representative pictures of Iba1 and

GFAP staining in ARC from Western diet-fed wild-type mice treated with antibiotics or placebo while administrated with vehicle or Ex9-39 (M). Scale bar: 100 μm. Body weight gain between surgery and end of the study (N), subcutaneous white adipose tissue (SC WAT) weight (O), epididymal white adipose tissue (eWAT) weight (P), and cecum weight (Q) were determined at the end of the experiment. All graphs show mean ± SEM. *, $P<0.05$, **, $P<0.01$ and ***, $P<0.001$ as determined by Mann-Whitney rank test in A-K, or by Kruskal-Wallis test in L-Q. CONV-R, conventionally raised; Abx, antibiotics; GF, germ-free; WD, Western diet; Lep, leptin; Veh, vehicle; Ex9-39, Exendin 9-39.

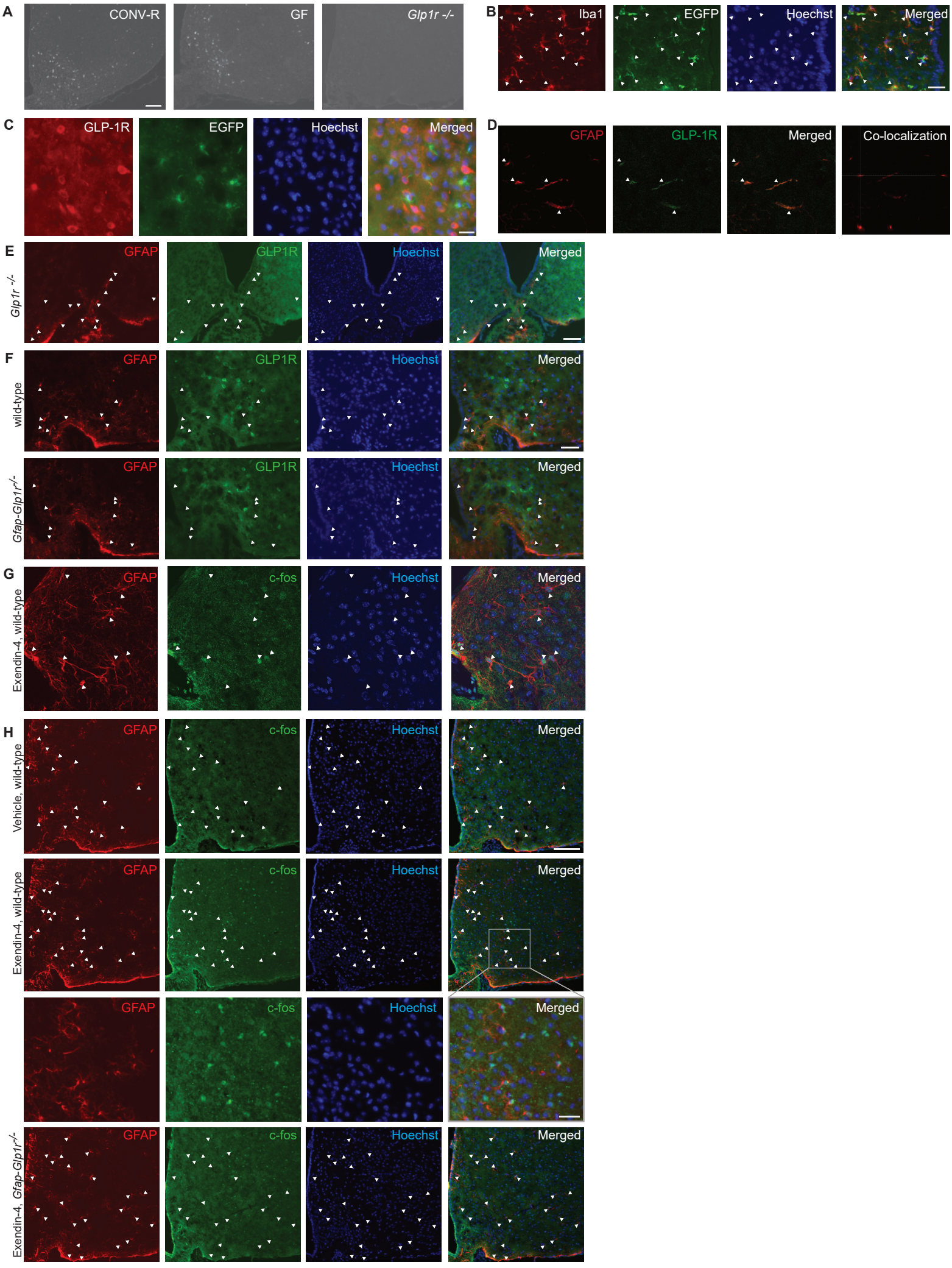
A
CONV-R
GF
Glp1r -/-
B
Iba1
EGFP
Hoechst
Merged
C
GLP-1R
EGFP
Hoechst
Merged
D
GFAP
GLP-1R
Merged
Co-localization
E
Glp1r -/-
GFAP
GLP1R
Hoechst
Merged
F
wild-type
Gfap-Glp1r-/-
GFAP
GLP1R
Hoechst
Merged
G
Exendin-4, wild-type
GFAP
c-fos
Hoechst
Merged
H
Vehicle, wild-type
Exendin-4, wild-type
Exendin-4, Gfap-Glp1r-/-
GFAP
c-fos
Hoechst
Merged

Figure S4. Deletion of GLP-1R in GFAP-expressing cells diminishes antibiotic-mediated protection against diet-induced hypothalamic inflammation. Related to Figure 4.

(A) GLP-1R staining of hypothalamic sections from CONV-R WT, GF WT and CONV-R *Glp1r* $^{-/-}$ mice. Scale bar: 100 µm. (B) Co-localization between Iba1 and EGFP in ROSA mTmG mice bred with mice expressing tamoxifen-inducible Cre under the Cx3cr1 promoter. Scale bar: 25 µm. (C) Co-localization between GLP-1R and EGFP in ROSA mTmG mice bred with mice expressing tamoxifen-inducible Cre under the Cx3cr1 promoter. Scale bar: 25 µm. (D) Co-localization was observed between GLP-1R and the astrocyte marker GFAP using a confocal microscope. (E) GFAP and GLP-1R immunostaining in *Glp1r* $^{-/-}$ mice. Scale bar: 100 µm. (F) Expression of GLP-1R in wild-type mice and in mice with specific deletion of the GLP-1R in the GFAP-positive cells. Scale bar: 50 µm. (G) Expression of c-fos in $GFAP^{+}$ astrocytes after Ex4 injection in fasted mice using confocal imaging. (H) c-fos-positive astrocytes after vehicle or Exendin-4 (10 µg/kg) i.p. injection in 12-hour fasted female mice. Scale bar: 100 µm, Scale bar in insert: 25 µm.

Mouse model	chow	2-days Western diet	1-week Western diet	4-weeks Western diet
CONV-R WT	Hypothalamic Iba1+ and GFAP+ cells Hypothalamic gene expression Colonic *Gcg* expression	Hypothalamic gene expression	Hypothalamic Iba1+ and GFAP+ cells Hypothalamic gene expression Plasma GLP-1, leptin and insulin measurements Leptin-induced hypothalamic pSTAT3 Leptin-induced effects on food intake Colonic *Gcg* expression GLP-1R immunofluorescence Ex9-39, AF12198 or Etanercept administration	Hypothalamic Iba1+ and GFAP+ cells Plasma GLP-1 measurements Hypothalamic gene expression
GF WT	Hypothalamic Iba1+ and GFAP+ cells Hypothalamic gene expression Colonic *Gcg* expression	Hypothalamic gene expression	Hypothalamic Iba1+ and GFAP+ cells Hypothalamic gene expression Plasma GLP-1 measurements Leptin-induced hypothalamic pSTAT3 Colonic *Gcg* expression GLP-1R immunofluorescence Ex9-39 administration	
Abx WT	Hypothalamic Iba1+ and GFAP+ cells Hypothalamic gene expression	Hypothalamic gene expression	Hypothalamic Iba1+ and GFAP+ cells Hypothalamic gene expression Plasma GLP-1, leptin and insulin measurements Leptin-induced hypothalamic pSTAT3 Leptin-induced effects on food intake GLP-1R immunofluorescence Ex9-39 administration	Hypothalamic Iba1+ and GFAP+ cells Plasma GLP-1 measurements
CONV-R *Glp-1r* KO	Hypothalamic Iba1+ and GFAP+ cells		Hypothalamic Iba1+ and GFAP+ cells Leptin-induced hypothalamic pSTAT3 GLP-1R immunofluorescence	
Abx *Glp-1r* KO	Hypothalamic Iba1+ and GFAP+ cells		Hypothalamic Iba1+ and GFAP+ cells Leptin-induced hypothalamic pSTAT3 GLP-1R immunofluorescence	
CONV-R *Gfap-Glp-1r* KO	Functional assay of GLP-1R depletion (Ex4 injection)		Hypothalamic Iba1+ and GFAP+ cells GLP-1R immunofluorescence	
Abx *Gfap-Glp-1r* KO	Functional assay of GLP-1R depletion (Ex4 injection)		Hypothalamic Iba1+ and GFAP+ cells GLP-1R immunofluorescence	

Table S1. Overview of the animal experiments performed. Related to STAR methods.